Zeyu Wang, Abdollah Shafieezadeh The Ohio State University, Columbus, OH, 43210, United States

Real-Time High-Fidelity Reliability Updating with Equality Information using Adaptive

ABSTRACT

Current state-of-the-art methods for reliability updating with equality information transform this challenging problem into an inequality one by introducing an auxiliary random variable. However, the joint event of information and failure in the derived conditional probabilities is typically very rare, and therefore, very challenging to estimate. Moreover, updating the reliability as new information arrives requires reevaluation of the probability of the joint event, which involves large numbers of calls to performance functions. We address these limitations by proposing a new approach to reliability updating called RUAK. One of the important contributions is the decomposition of the rare joint event of the failure and observed information into two events both with relatively high probabilities. Moreover, an adaptive Kriging-based reliability analysis method is proposed for the estimation of the prior failure probability and the conditional probability of information. This way, reliability updating for new information is conducted using the efficient Kriging meta-model, which significantly enhances the computational efficiency. Results for four examples indicate that the computational demand using RUAK is decreased by two orders of magnitude compared to the state-of-the-art methods, while achieving higher accuracy. This approach facilitates real-time reliability updating for various applications such as health monitoring and warning systems.

Key words: Reliability updating; reliability analysis; surrogate model; adaptive Kriging; Poisson Binomial distribution; measurement errors; monitoring

1. Introduction

As sensing technologies are maturing and becoming more cost efficient, allowing their implementation at large scales, information about the state of the built and natural environments are becoming more available. These observations can include, for example, data on external loadings, component- and system-level responses, and changes in characteristics of the systems. This information can be leveraged to reevaluate or update forecasts of the performance of these systems. Among many metrics, reliability is one of the most capable system performance measures that quantifies the probability of meeting a performance objective considering the set of uncertainties that influence the performance. Updating reliability estimates based on information provided by sensing systems can enhance confidence in our forecasts of the future performance of the systems and lead to more effective risk-informed decisions.

Let X denote the vector of random variables with n dimensions, $\rho(x)$ represent the joint probability density function of x in X, E denote the events (i.e., failure in reliability analysis) and Z_i represent the ith observation obtained from sensors or monitoring equipment. Ω_E and Ω_{Z_i} are the domains corresponding to the outcome space of X. Concerning information $Z = \{Z_1 \cap Z_2 ... \cap Z_m\}$, where m is the number of information pieces, the conditional probability $\Pr(E|Z)$ can be defined as:

$$\Pr(E|Z) = \frac{\Pr(E \cap Z)}{\Pr(Z)} = \frac{\int_{x \in \{\Omega_E \cap \Omega_{Z_1} \cap \dots \cap \Omega_{Z_m}\}} \rho(x) dx}{\int_{x \in \{\Omega_{Z_1} \cap \dots \cap \Omega_{Z_m}\}} \rho(x) dx}$$
(1)

 Moreover, let the vector of random variables, X in Eq. (1) be partitioned into two groups of random variables X_g and X_h . Here, X_h denotes the random variables that appear in the information, Z_i , exclusively and X_g represents the remaining variables in X. In reliability analysis, the prior probability of the failure event, denoted as Pr(E) or P_f can be determined as:

$$P_f = P(g(\mathbf{X}_g) \le 0) = \int_{\mathbf{X}_g \in \Omega_E} \rho(\mathbf{X}_g) d\mathbf{x}$$
 (2)

2

4

5

6

7

8

9

10

11 12

13

14 15

16

17

18 19

20

21 22

23

24 25

26

27 28

29

30

31 32

33

34

35 36

37

38

39

40 41

42

43

44

45

46 47

48

Methods for computing the prior failure probability include but are not limited to: crude Monte Carlo simulations (MCS) [1], [2], First and Second Order Reliability Methods (FORM & SORM) [3], [4], Importance Sampling [5], Subset Simulation [6], [7], and surrogate model-based approaches [8]–[14]. Among these methods, two Kriging-based approaches, AK-MCS proposed by Echard et al. [8] and EGRA proposed by Bichon et al. [15], have shown great computational efficiency and hence attracted considerable attention. To further enhance Kriging-based reliability analysis, improvements to active learning functions, learning stopping criteria, and sampling strategies have been proposed. With regard to active learning functions, the expected feasible function (EFF) is proposed by Bichon et al. [15], which prioritizes points with large uncertainty and those that are close to the limit state. On the other hand, the 'U' learning function proposed by Echard et al. [8] aims to quantify the probability of wrong sign estimation, which has been adopted in recent publications [5], [16], [17]. Similar to 'EFF', an information entropy-based learning function 'H', is developed by Lv et al. [18]. Moreover, Sun et al. [19] proposed the Least Improvement Function 'LIF', which improves the learning process by searching for next best training points with high probability of wrong sign estimation in the vicinity of the limit state, and gives higher priority to points with high probability density. Other state-of-the-art learning functions are also shown to be very efficient in strategically searching for training samples [20], [21]. However, aforementioned active learning methods can just select one training point upon each iteration. A number of parallel training strategies, such as kmeans clustering and pseudo-Kriging, have been investigated in [12], [22]-[24]. For stopping criteria, Bichon et al. [15] and Wen et al. [23] set the maximum EFF smaller than a prescribed threshold (e.g., $max(EFF) \le 0.001$) as the indication of convergence. Additionally, the stopping criterion $min(U) \ge$ 2 has been used in many studies [5], [8], [16], [17], [25]. It is shown that both stopping criteria $max(EFF) \le 0.001$ and $min(U) \ge 2$ may lead to a relatively large number of unnecessary trainings of the surrogate model [8], [26]-[28]. Gaspar et al. [27] proposed a new stopping criterion based on the stability of the estimated failure probability. Fauriat et al. [26] points out that the Kriging model is sufficiently accurate if 98% of the candidate design samples satisfy $min(U) \ge 2$. By deriving the maximum error of estimated probability of failure, Wang and Shafieezadeh [29] proposed an efficient stopping criterion for the Kriging-based reliability analysis. An approach for real-time estimation of the maximum error for time-dependent reliability analysis was developed by Jiang et al [30]. For sampling strategies, Echard et al. [5], Balesdent et al. [31] and Dubourg et al. [32] used importance sampling techniques in association with the adaptive Kriging model, which facilitates reliability analysis for rare events. Moreover, Zhang et al. proposed the AKOIS method to optimize the procedure of searching for importance sampling center, which is an efficient technique for circumstances with multiple Most Probable Points (MPPs) [33]. Chen et al. [34] developed a strategy that replaces the original sample population with multiple equivalent ones. Such a strategy enhances the learning process with sufficient candidate deign samples in the vicinity of the limit state. Additionally, subset simulation techniques are used with Kriging-based reliability analysis in [16], [35] [36]. For example, Zhang et al. [37] proposed that the failure region can be better explored by combining the Kriging meta-model with subset simulation. Wen et al. [23], Yang et al. [20] and Wang and Shafieezadeh [38] proposed truncated candidate samples regions, which cut off candidate samples with small values of probability density. Through this approach, the number of evaluations of the performance function can be significantly reduced. To enable the Kriging-based reliability analysis for high-dimensional problems, several strategies have been proposed including sensitivity analysis-based methods [28], [39], [40] and dimension reduction-based techniques [41]. These methods have also been extended to efficiently solve time-variant reliability analysis problems by transforming these limit state function into timeinvariant ones. The method subsequently takes the minimum value of all the responses at all time discretizations [17], [42], [43]. Moreover, the system reliability analysis has been improved significantly using Kriging surrogate models [20], [26], [44]. It is shown that Kriging can be integrated in the reliability

quantification (UQ) techniques such as Bayesian updating [48], [49].

While various approaches for estimating the prior failure probability have been proposed, methods for computing the posterior failure probability, denoted as B' bereby, are still under developed. It is known that

 while various approaches for estimating the prior failure probability have been proposed, methods for computing the posterior failure probability, denoted as P'_f hereby, are still under-developed. It is known that the computational complexity of estimating P'_f depends primarily on the category of information [50]: inequality or equality. The information Z_i can be categorized as inequality, if it can be expressed as:

sensitivity analysis [45], reliability-based design optimization [46], [47] and other uncertainty

$$\Omega_{Z_i} = \{ h_i(\mathbf{x}) \le 0 \} \tag{3}$$

where $h_i(x)$ denotes the *i*th information function. On the other hand, information is classified into the equality group, if it can be represented as:

$$\Omega_{Z_i} = \{ h_i(\mathbf{x}) = 0 \} \tag{4}$$

The reliability analysis methods for estimating P_f in Eq. (2) can also be used to solve reliability updating with inequality information in Eq. (3). However, reliability updating with equality information is relatively intractable because the integrals in Eq. (1) result in zero probability, which cannot be treated as the denominator. To overcome this challenge, integrals in Eq. (1) can currently only be solved using the surface integral technique [50], which, however, is challenging to implement and cannot take advantage of the well-developed reliability analysis methods.

To address these limitations, a number of techniques have been proposed that leverage existing reliability analysis procedures to solve reliability updating with equality information. Gollwitzer et al. [51] integrated the surface integral method with FORM & SORM techniques, which offers acceptable efficiency and accuracy for linear reliability problems. However, the performance of this approach is not satisfactory when the problem is non-linear, as the identification of the Most Probable Point (MPP) in such problems using FORM/SORM may not be accurate. Alternatively, P_f' can be estimated as a partial derivative by introducing a dummy variable Δ as follows [50]:

$$P_f' = \Pr(g(\mathbf{X}_g) \le 0 | h(\mathbf{X}) = 0) = \frac{\Pr[g(\mathbf{X}_g) \le 0 \cap h(\mathbf{X}) = 0]}{\Pr[h(\mathbf{X}) = 0]}$$

$$= \frac{\lim_{\Delta \to 0} \frac{\partial}{\partial \Delta} \Pr[g(\mathbf{X}_g) \le 0 \cap h(\mathbf{X}) - \Delta \le 0]}{\lim_{\Delta \to 0} \frac{\partial}{\partial \Delta} \Pr[h(\mathbf{X}) - \Delta \le 0]}$$
(5)

This way, the equality information $\{h(x) = 0\}$ is transformed into an inequality, which means that existing reliability analysis techniques can be applied. However, this approach in conjunction with FORM & SORM can potentially result in significant errors in estimates of P_f' , as the use of partial derivatives can amplify the error estimated by the FORM & SORM. Another powerful tool called Bayesian Networks (BNs) is widely used for reliability updating purposes. Straub and Luque [52], [53] integrated a Dynamic Bayesian Network (DBN) and successfully applied it to time-invariant and time-variant deterioration problems. DBNs are successfully applied in tunnel excavation [54], life-cycle analysis [55] and bridge condition prediction [56]. However, generating the conditional probability tables (potentials), which are a crucial part in BNs-based reliability updating, is very computationally demanding. To address this challenge, Straub and Der Kiureghian [57], [58] proposed an enhanced BN framework denoted as eBN/rBN. In this approach, the potentials are generated based on the reduced BNs (rBNs) with only discrete nodes by defining the Markov envelop and strategically eliminating all the continuous nodes in eBN. Existing exact inference algorithms can then be applied to update reliability based on the produced potentials table. The eBN/rBN

are used in post-earthquake risk analysis and decision making [59]. A number of other investigations have also used BNs for reliability updating [60]-[63]. However, BN-based approaches for reliability updating have a number of limitations. First, the number of evaluations of the performance function q(X), which is typically time-consuming e.g. for the case of high-fidelity Finite Element Models (FEMs), is still very large; this limitation hampers the application of eBN/rBN for engineering and science problems. Furthermore, the procedure for constructing the eBN/rBN is very complex and cannot be conducted by non-experts, as it requires empirical knowledge of the process for node elimination and discretization. In contrast to the BNbased reliability updating methods, Straub [50] proposed a new solution by reformulating the equality information $\{h_i(x) = 0\}$ into an inequality information $\{h_i(x^*) \le 0\}$ with an additional auxiliary standard normal random variable. By solving two structural reliability problems, this method enables reliability updating without discretizing the outcome space of the information. This newly developed method has been implemented in a number of practical engineering problems including fatigue-induced crack growth [50], geotechnical engineering [64], [65], and system reliability updating [66]. However, this approach has two shortcomings. The joint event in the numerator of the equation of conditional probability is very often a rare event, which makes the conventional reliability analysis methods such as FORM or SORM inefficient and inaccurate. Moreover, when new information becomes available, reliability analyses need to be repeated in order to estimate the new probability of the joint event of observed information and failure. These unavoidably increase the number of evaluations of the performance function and reduce the accuracy of the reliability updating outcomes.

To overcome the aforementioned limitations, a new reliability updating method based on surrogate models called Reliability Updating using Adaptive Kriging (RUAK) is proposed. A key contribution here that facilitates computationally efficient reliability updating is the decomposition of P'_f into three parts using the Bayes' theorem: prior failure probability $Pr(E) = P_f$, probability of information Pr(Z), and conditional probability of information Pr(Z|E). Unlike calculating the joint probability $Pr(E \cap Z)$ in [50], which is typically a rare event, Pr(E) and Pr(Z|E) are proposed to be estimated separately by surrogate model-based reliability analysis methods, since these events have considerably higher likelihood. A general approach based on surrogate models is then proposed to accurately and efficiently estimate the prior failure probability P_f . This is achieved by generating a well-trained surrogate model that substitutes the original time-consuming performance model and therefore allows the estimation of the failure probability using crude MCS or Markov Chain Monte Carlo (MCMC). Another important feature of RUAK is that it leverages the generated surrogate model to estimate Pr(Z|E) by introducing an auxiliary uniform random variable. Later in the article, an adaptive Kriging-based reliability analysis method [8], [15] enhanced with a new training stopping criterion called ESC is proposed as the surrogate model. RUAK offers several advantages compared with conventional and state-of-the-art approaches. First, the reliability updating problem involves estimation of P_f , which is rather straightforward. Second, only one reliability analysis for P_f and P_f' is needed throughout the updating process when new information becomes available. This feature dramatically reduces the number of evaluations of the performance function. It should be noted that this paper only investigates the feasibility of applying the surrogate model in reliability updating, thus, the optimal surrogate model and other strategies for accuracy improvements are not discussed in this paper.

A brief review of reliability updating with equality information is provided in Section 2. A new approach for reliability updating with equality information using surrogate models is introduced in Section 3. In Section 4, the proposed method RUAK is presented. This method is applied to four numerical examples in Section 5. Finally, conclusions are presented in Section 6.

2. Reliability updating

1

2

4

5 6

7

8

9

10

11 12

13

14

15

16

17

18 19

20

21

22

23

24 25

26 27

28 29

30

31 32

33

34

35 36 37

38

39

40 41

42

43

44 45

46

47 48

49

According to Eq. (1), reliability updating is the process of estimating the posterior failure probability i.e., denoted as Pr(E|Z) or P'_f where $P'_f = Pr(E \cap Z)/Pr(Z)$ and E represents the failure event, based on existing information, Z. To accurately estimate P'_f based on equality information without discretizing the information space, Straub [50] proposed an innovative approach by transforming the equality information

into an equivalent inequality function. In this section, the method used in [50] is briefly described, then a new method based on surrogate models is proposed in the following section.

For information obtained for a system, there exists a likelihood function L(x) with the following property [50], [67]:

$$L(\mathbf{x}_g) \propto Pr(Z|\mathbf{X}_g = \mathbf{x}_g) \tag{6}$$

where x_g is the realization of the random vector X_g . To further elaborate the above formulation, let's consider a case where Z represents the measurement s_m of a property of the system s(x) with measurement error ε . Thus, the likelihood function can be represented as $L(x_g) = f_{\varepsilon}[s_m - s(x_g)]$, with f_{ε} being the probability density function (PDF) of ε , and X_g denotes all variables in X except ε . For this case, $x_h = \varepsilon$ and $h_i(x) = 0$ can be represented in the form of $h(x_g, \varepsilon) = s(x_g) - s_m + \varepsilon$. Based on this likelihood function, the following equation always holds:

$$L(\mathbf{x}_g) = \frac{1}{c} \Pr\{\mathcal{N} - \Phi^{-1}[cL(\mathbf{x}_g)] \le 0\}$$
 (7)

where $\mathcal N$ is a standard normal random variable, Φ^{-1} is the inverse of the standard normal cumulative distribution function (CDF) and c is a constant satisfying $0 \le cL(\mathbf x_g) \le 1$. Note that $\frac{1}{c}\Pr\{\mathcal N - \Phi^{-1}[cL(\mathbf x_g)] \le 0\} = \frac{1}{c}\Phi\{\Phi^{-1}[cL(\mathbf x_g)]\} = L(\mathbf x_g)$. Therefore, with Eq. (7), the formulation of the likelihood function $L(\mathbf x_g)$ is transformed into a reliability analysis problem with the limit state function represented as:

$$h(n, \mathbf{x}_g) = n - \Phi^{-1}[cL(\mathbf{x}_g)] \tag{8}$$

with the acceptable domain defined as $\Omega_{\hat{Z}} = \{ \mathcal{N} - \Phi^{-1}[cL(x_g)] \le 0 \}$. Considering Eq. (8), it can be shown that:

$$\Pr(Z|X_g = x_g) = \frac{a}{c} \int_{x_g, n \in \Omega_{\widehat{Z}}} \varphi(n) \, dn \tag{9}$$

where $\varphi(\cdot)$ is the probability density function of the standard normal distribution and a is a constant for considering the proportional relation in Eq. (6). Thus, the probability of the evidence can be derived as:

$$Pr(Z) = \int_{x_g \in \Omega} Pr(Z | X_g = x_g) \rho(x_g) dx_g$$

$$= \frac{a}{c} \int_{x_g, n \in \Omega_Z} \varphi(n) \rho(x_g) dn dx_g$$
(10)

where Ω is the output space of the random variable X_g . Accordingly, the probability of the joint event $Pr(E \cap Z)$ can be derived as:

$$\Pr(E \cap Z) = \int_{\mathbf{x}_g \in \Omega} \Pr(E | \mathbf{X}_g = \mathbf{x}_g) \Pr(Z | \mathbf{X}_g = \mathbf{x}_g) \rho(\mathbf{x}_g) d\mathbf{x}_g$$

$$= \frac{a}{c} \int_{\mathbf{x}_g, n \in \{\Omega_{\widehat{g}} \cap \Omega_E\}} \varphi(n) \rho(\mathbf{x}_g) dn d\mathbf{x}_g$$
(11)

Hence, the conditional failure probability in Eq. (1) can be rewritten as:

$$\Pr(E|Z) = \frac{\Pr(E \cap Z)}{\Pr(Z)} = \frac{\int_{x_g, n \in \{\Omega_{\widehat{Z}} \cap \Omega_E\}} \varphi(n) \rho(x_g) \, dn \, dx_g}{\int_{x_g, n \in \Omega_{\widehat{Z}}} \varphi(n) \rho(x_g) \, dn \, dx_g}$$
(12)

Denoting the random variables $[x_g, n]$ as x^* , the above equation can be represented as:

$$\Pr(E|Z) = \frac{\int_{\mathbf{x} \in \{\Omega_{\widehat{Z}} \cap \Omega_{E}\}} \rho^{*}(\mathbf{x}^{*}) d\mathbf{x}^{*}}{\int_{\mathbf{x} \in \Omega_{\widehat{Z}}} \rho^{*}(\mathbf{x}^{*}) d\mathbf{x}^{*}}$$
(13)

where $\rho^*(x^*) = \varphi(n)\rho(x_g)$ is the PDF of the new random variable x^* . The method derived in Eq. (13) enables updating reliability without any assumption or approximation just by solving two reliability problems. It achieves sufficient accuracy and efficiency with MCS-based approaches as shown in [50]. However, there are still some drawbacks in this approach. Obviously, in the numerator of Eq. (13), two limit state functions need to be investigated including the performance function $g(X_g)$ and the limit state function in Eq. (8). Additionally, the numerator of Eq. (13) is concerned with the analysis of a series system reliability problem with two limit state functions, which is typically a rare event with very small probability. Non-MCS-based reliability analysis techniques such as FORM or SORM are not reliable for such circumstances. Moreover, it is necessary to reevaluate the numerator in Eq. (13) whenever new information become available, which unavoidably increases the number of evaluations of the performance function $g(X_g)$. This process becomes very time-consuming when the performance function $g(X_g)$ involves a complex numerical model such as a high-fidelity FEM. To overcome the aforementioned limitations, an efficient surrogated-based reliability updating algorithm called RUAK is proposed in the next section.

3. Reliability updating using surrogate models

Here we propose decomposing the posterior failure probability P'_f into three parts using Bayes' theorem: prior failure probability P_f , probability of information Pr(Z), and conditional probability of information Pr(Z|E):

$$P'_f = \Pr(E|Z) = \frac{\Pr(Z|E) \cdot \Pr(E)}{\Pr(Z)} = \frac{\Pr(Z|E) \cdot P_f}{\Pr(Z)}$$
(14)

Note that the formulation of reliability updating through Bayes' theorem in Eq. (14) is different from the approach presented in Eq. (1), which is based on the joint event i.e., $P'_f = \Pr(E \cap Z)/\Pr(Z)$. Derivations and computational details of P_f (Eq. (16)-(17)) and $\Pr(Z|E)$ (Eq. (18)-(21)) are presented in the rest of this section. First, $\Pr(Z)$ can be determined in a similar fashion to that in [50] using Equation (7)-(10). The

problem in Eq. (7) can be reformulated in a simpler way using an auxiliary standard uniform distribution instead of a normal distribution:

$$L(x_g) = \frac{1}{c_1} \Pr\{P - c_1 L(x_g) \le 0\}$$
 (15)

- where P is a standard uniform random variable, c_1 is a constant satisfying $0 \le c_1 L(x_g) \le 1$, and it is recommended that $c_1 = \frac{1}{max(L(x_g))}$. Note that both normal and uniform auxiliary variables are able to
- transfer the equality information to inequality information. To make the derivation of reliability updating with equality information mathematically simpler, a uniform auxiliary random variable is used in this article. Estimation of Pr(Z) follows the process presented in Eq. (10), but based on the limit state function

 $h^+(p, \mathbf{x}_g) = p - c_1 L(\mathbf{x}_g).$

The prior probability of failure, P_f , can be estimated using MCS:

$$P_f = \frac{\sum_{i=1}^{N_{MCS}} I_g\left(\mathbf{x}_{g_i}\right)}{N_{MCS}}, \mathbf{x}_{g_i} \in S$$
(16)

- where N_{MCS} is the number of the samples for MCS, x_{g_i} denotes the realizations of random variable X_g , S_g represents all the samples for MCS, and $I_g(\cdot)$ is the indicator function for the responses from the
- 15 performance function $g(x_{g_i})$:

$$I_g\left(\mathbf{x}_{g_i}\right) = \begin{cases} 1, & \text{when } g(\mathbf{x}_{g_i}) \le 0\\ 0, & \text{when } g(\mathbf{x}_{g_i}) > 0 \end{cases}$$
 (17)

The proposed reliability updating formulation in Equation (14) involves the new term Pr(Z|E). This probability can be derived as:

$$\Pr(Z|E) = \int_{\mathbf{x}' \in \Omega_f} \Pr(Z|\mathbf{X}' = \mathbf{x}') \rho'^{(\mathbf{x}')} d\mathbf{x}'$$

$$= \frac{a}{c_2} \int_{\mathbf{x}', p \in \Omega_{Z^{++}}} \psi(p) \rho'(\mathbf{x}') dp d\mathbf{x}' = \frac{a}{c_2} \int_{\mathbf{x}', p \in \Omega_{Z^{++}}} \rho'(\mathbf{x}') dp d\mathbf{x}'$$
(18)

where X' is the random variable with the posterior distribution of X_g in the failure domain Ω_f , x' is the realization of X', $\psi(\cdot)$ is the PDF of the standard uniform distribution, ρ' is the PDF of X', c_2 is a constant satisfying $0 \le c_2 L(x') \le 1$, and is determined as $c_2 = \frac{1}{max(L(x'))}$. Note that c_2 , which is a function of x', is not equal to c_1 which is a function of x_g in Eq. (15). $\Omega_{Z^{++}}$ is the acceptable domain corresponding to the following limit state function:

$$h^{++}(p, x') = p - c_2 L(x') \tag{19}$$

 $\Omega_{Z^{++}}$ can be subsequently defined as $\Omega_{Z^{++}} = \{h^{++}(p, \mathbf{x}') \leq 0\}$. Let $\widehat{\Omega}_f$ and $\widehat{\Omega}_S$ denote the estimated failure and safe domains in S, therefore, $\Pr(Z|E)$ can be calculated using MCS as follows:

$$\Pr(Z|E) = \frac{a}{c_2} \cdot \frac{\sum_{j=1}^{N_f} I_{Z^{++}}(\boldsymbol{x}_j', p_j)}{N_f}, \quad \boldsymbol{x}_j' \in \widehat{\Omega}_f$$
 (20)

where N_f denotes the number of samples in S_f , and $I_{Z^{++}}(\cdot)$ is the indicator function defined as:

$$I_{Z^{++}}(x'_j, p_j) = \begin{cases} 1, & \text{when } h^{++}(x'_j, p_j) \le 0\\ 0, & \text{when } h^{++}(x'_i, p_j) > 0 \end{cases}, \quad x'_j \in \widehat{\Omega}_f$$
 (21)

 Considering that the same unknown constant a appears in both Pr(Z) in Eq. (10) and Pr(Z|E) in Eq. (20), it is automatically eliminated in the subsequent computation in Eq. (14).

To implement the new approach most efficiently and accurately, we propose using surrogate model-based reliability analysis methods. Generally, this surrogate model represented by $\hat{g}(X_g)$ replaces $g(X_g)$ in the above equations to arrive at the posterior failure probability \hat{P}_f' . Different from the approach in [50] i.e. Eq. (13), in the proposed method, only the computation of \hat{P}_f requires the analysis of the performance function $g(X_g)$. As the surrogate model-based reliability algorithms are known for their capabilities to reduce the number of evaluations of the performance function, a well-trained surrogate model can be used to replace the originally time-consuming computational model. Moreover, with the new information, the computation of $\Pr(Z|E)$ in Eq. (20) is straightforward with minimal computational demand, as running only the surrogate model is required. However, in Eq. (13), one needs to reevaluate the performance function $g(X_g)$ for any new information that becomes available. Therefore, the proposed method derived from the Bayes' theorem has two primary advantages over the approach in [50]: (1) estimations of P_f and $\Pr(Z|E)$ are considerably less challenging than the probability of the joint event in the numerator of Eq. (13); and (2) once P_f is estimated, reliability updating for new information becomes highly efficient since the simulations can be conducted entirely on the well-trained surrogate model.

4. The RUAK algorithm

In this section, the proposed reliability updating method RUAK is presented. RUAK integrates the method presented in Section 3 with Kriging meta-model, which substitutes the originally time-consuming performance function $g(X_g)$ with a Kriging-based surrogate model $\hat{g}(X_g)$. The implementation of RUAK is explained step-by-step in the next sub-sections.

4.1 Kriging model

To estimate the prior failure probability P_f and $\Pr(Z|E)$, a surrogate model $\hat{g}(X_g)$ for the performance function $g(X_g)$ is constructed in this paper using the Kriging meta-model. The Kriging meta-model, also known as the Gaussian Process Regression, has been widely used in computer-based experiment design [68]. In this model, the estimated responses are mean values and variances following a normal distribution [39], [68]. An extensive review of the Kriging surrogate model can be found in [68]–[70]. In Kriging, $\hat{g}(X_g)$ is defined as:

$$\hat{g}(\mathbf{X}_g) = F(\boldsymbol{\beta}, \mathbf{X}_g) + \psi(\mathbf{X}_g) = \boldsymbol{\beta}^T \mathbf{B}(\mathbf{X}_g) + g p(\mathbf{X}_g)$$
(22)

 where \mathbf{x} is the vector of random variables, $F(\boldsymbol{\beta}, \mathbf{x}_g)$ are the regression elements, and $gp(\mathbf{x}_g)$ is the Gaussian process. In $F(\boldsymbol{\beta}, \mathbf{x}_g)$, $\mathbf{B}(\mathbf{x}_g)$ is the Kriging basis and $\boldsymbol{\beta}$ is the corresponding set of coefficients. There are multiple formulations of $\boldsymbol{\beta}^T \mathbf{B}(\mathbf{x}_g)$ including ordinary (β_0) , linear $(\beta_0 + \sum_{i=1}^N \beta_i \mathbf{x}_i)$, or quadratic $(\beta_0 + \sum_{i=1}^N \beta_i \mathbf{x}_i + \beta_0 + \sum_{i=1}^N \sum_{j=1}^i \beta_{ij} \mathbf{x}_i \mathbf{x}_j)$, where N is the number of dimensions of \mathbf{x}_g . In this article, the ordinary Kriging model is used. The Gaussian process $gp(\mathbf{x}_g)$ has a zero mean and a covariance matrix that can be represented as:

$$COV\left(g_{\mathcal{P}}(\mathbf{x}_i), g_{\mathcal{P}}(\mathbf{x}_i)\right) = \sigma^2 R(\mathbf{x}_i, \mathbf{x}_i; \boldsymbol{\theta})$$
(23)

where σ^2 is the process variance or the generalized mean square error (MSE) from the regression, x_i and x_j are two observations, and $R(x_i, x_j; \theta)$ is known as the kernel function representing the correlation between observations x_i and x_j parametrized by θ . The correlation functions implemented in Kriging can include, among others, linear, exponential, Gaussian, and Matérn functions. The Gaussian kernel function is used in this paper, which has the following form:

$$R(\mathbf{x}_i, \mathbf{x}_j; \boldsymbol{\theta}) = \prod_{k=1}^{N} \exp\left(-\theta^k \left(x_i^k - x_j^k\right)^2\right)$$
 (24)

where x_i^k is the k_{th} dimension of x_i and θ is estimated via the Maximum Likelihood Estimation (MLE) method [68]. It is shown that the variation of θ has significant impact on the performance of the Kriging meta-model [23], [71], [72]. To maintain consistency, θ^k is searched in (0,10) using the optimization algorithms in DACE [69], [73] or UQLab [68]. Here, the formulation based on MLE can be presented as:

$$\boldsymbol{\theta} = \underset{\boldsymbol{\theta}^*}{\operatorname{argmin}} \left(\left| \boldsymbol{R}(\boldsymbol{x}_i, \boldsymbol{x}_j; \boldsymbol{\theta}^*) \right|^{\frac{1}{m}} \sigma^2 \right)$$
 (25)

where m is the number of training points. Accordingly, the regression coefficient β , and the predicted mean and variance can be determined as follows [68]:

$$\boldsymbol{\beta} = (\boldsymbol{F}^{T}\boldsymbol{R}^{-1}\boldsymbol{F})^{-1}\boldsymbol{F}^{T}\boldsymbol{R}^{-1}\boldsymbol{Y}$$

$$\mu_{\hat{g}}(\boldsymbol{x}_{g}) = \boldsymbol{B}^{T}(\boldsymbol{x}_{g})\boldsymbol{\beta} + \boldsymbol{r}^{T}(\boldsymbol{x}_{g})\boldsymbol{R}^{-1}(\boldsymbol{y} - \boldsymbol{F}\boldsymbol{\beta})$$

$$\sigma_{\hat{g}}^{2}(\boldsymbol{x}_{g}) = \sigma^{2}\left(1 - \boldsymbol{r}^{T}(\boldsymbol{x}_{g})\boldsymbol{R}^{-1}\boldsymbol{r}(\boldsymbol{x}_{g}) + \left(\boldsymbol{F}^{T}\boldsymbol{R}^{-1}\boldsymbol{r}(\boldsymbol{x}_{g}) - \boldsymbol{B}(\boldsymbol{x}_{g})\right)^{T}(\boldsymbol{F}^{T}\boldsymbol{R}^{-1}\boldsymbol{F})^{-1}\left(\boldsymbol{F}^{T}\boldsymbol{R}^{-1}\boldsymbol{r}(\boldsymbol{x}_{g}) - \boldsymbol{B}(\boldsymbol{x}_{g})\right)\right)$$
(26)

where F is the matrix of the basis function $B(x_g)$ evaluated at the training points, i.e., $F_{ij} = B_j(x_i)$, i = 1, 2, ..., m; j = 1, 2, ..., p, $r(x_g)$ is the correlation between known training points x_i and an untried point x_g : $r_i = R(x_g, x_i, \theta)$, i = 1, 2, ..., m, and R is the autocorrelation matrix for known training points: $R_{ij} = R(x_i, x_j, \theta)$, i = 1, 2, ..., m; j = 1, 2, ..., m. Therefore, $\hat{g}(x_g)$ can be presented using the estimated Kriging mean $\mu_{\hat{g}}(x_g)$ and variance $\sigma_{\hat{g}}^2(x_g)$ as:

$$\hat{g}(x_g) \sim N\left(\mu_{\hat{g}}(x_g), \sigma_{\hat{g}}^2(x_g)\right) \tag{27}$$

It is obvious that the responses from the Kriging model $\hat{g}(x_g)$ are not deterministic but probabilistic in the form of a normal distribution with mean $\mu_{\hat{g}}(x_g)$ and variance $\sigma_{\hat{g}}^2(x_g)$. This stochastic property allows developing strategies for enriching the training points by refining the Kriging model. In the following subsection, the framework of RUAK and the implementation steps are explained.

4.2 RUAK

The proposed RUAK algorithm is described in this section, and a flowchart illustrating the process is presented in Fig 1. The details of each step are summarized below:

• Step 1: Generating initial candidate design samples. In this step, N_{MCS} candidate design samples are

generated by Latin Hypercube Sampling (LHS) and the set of samples is denoted as S.

• Step 2: Initial training points. Randomly select an initial set of training points denoted as x_{tr} from S. The number of initial training points affects the quality of the initial Kriging model and the computational demand of the reliability analysis. For similar problems to those considered in this paper, the study in [8] indicated that 12 initial training points are adequate. Therefore, we have used this number in the studies in this article.

• Step 3: Kriging construction. Construct the Kriging meta-model $\hat{g}(X_g)$ with current training points x_{tr} . This construction can be based on available packages such as DACE [69], [73] or UQLab [68]. Here, an ordinary Kriging basis and Gaussian correlation function are used.

• Step 4: Kriging prediction. The Kriging responses $\mu_{\hat{g}}(x_g)$ and variances $\sigma_{\hat{g}}^2(x_g)$ are obtained from the current Kriging model $\hat{g}(X_g)$ for every point in S. According to responses $\mu_{\hat{g}}(x_g)$, the failure probability \hat{P}_f is estimated by crude MCS.

• Step 5: *Identification of the next training point.* In this stage, the popular 'U' learning function is implemented to search for the next best training point. The 'U' learning function has the following form:

$$U(\mathbf{x}_g) = \frac{|\mu_K(\mathbf{x}_g)|}{\sigma_K(\mathbf{x}_g)}$$
 (28)

The 'U' learning function estimates the probability that $\hat{g}(x_g)$ wrongly estimate the sign (+/-) of the performance function at x_g . Thus, the point that minimizes the response of the 'U' learning function is selected as the next best training point:

$$\mathbf{x}_{tr}^* = \min_{\mathbf{x}_g \in S} (U) \tag{29}$$

• Step 6: Updating the training points. Add the next training point to the set of training points.

 • Step 7: Maximum error estimation of \hat{P}_f . As stated in the introduction, the conventional stopping criteria (e.g. $Min(U) \ge 2$) are often too conservative and lead to unnecessary over-training of the surrogate models. To resolve this issue, an efficient stopping criterion developed by the authors in [29] is adopted here. First, the maximum error $\hat{\epsilon}_{max}$ of the estimated prior failure probability is determined. Note that the failure probability with the Kriging model can be computed as:

$$\hat{P}_f = \frac{\hat{N}_f}{N_{mcs}} \tag{30}$$

where \widehat{N}_f is the estimated number of failure points in *S*. The true failure probability based on crude MCS is:

$$P_f = \frac{N_f}{N_{mcs}} \tag{31}$$

where N_f is the true number of failure points. Thus the relative error of \hat{P}_f can be defined as:

$$\epsilon = \left| \frac{\hat{P}_f}{P_f} - 1 \right| = \left| \frac{\hat{N}_f - N_f}{N_f} \right| \tag{32}$$

The estimated failure domain is denoted as $\widehat{\Omega}_f$, the safe domain as $\widehat{\Omega}_s$, the total number of wrong sign estimations in $\widehat{\Omega}_f$ as \widehat{S}_f , and in $\widehat{\Omega}_s$ as \widehat{S}_s . Note that $\widehat{\Omega}_f$, $\widehat{\Omega}_s \in \Omega$, and $\widehat{\Omega}_f \cap \widehat{\Omega}_s = \emptyset$. In the Kriging model, N_f , \hat{S}_s , and \hat{S}_f are not deterministic but follow Poisson binomial distributions as shown in [29]. N_f can therefore be estimated as:

$$N_f = \hat{N}_f + \hat{S}_S - \hat{S}_f \tag{33}$$

Here, both \hat{S}_s and \hat{S}_f follow a Poisson binomial distribution with mean and variance shown below [29]:

$$\hat{S}_{s} \sim PB\left(\sum_{i=1}^{\hat{N}_{s}} P_{i}^{wse}, \sum_{i=1}^{\hat{N}_{s}} P_{i}^{wse} \left(1 - P_{i}^{wse}\right)\right), x_{i} \in \widehat{\Omega}_{s}$$

$$(34)$$

$$\hat{S}_{f} \sim PB\left(\sum_{i=1}^{\hat{N}_{f}} P_{i}^{wse}, \sum_{i=1}^{\hat{N}_{f}} P_{i}^{wse} \left(1 - P_{i}^{wse}\right)\right), x_{i} \in \hat{\Omega}_{f}$$

$$(35)$$

where PB denotes the Poison Binomial distribution and P_i^{wse} denotes the probability of wrong sign

- estimation for x_i , which can be computed as $P_i^{wse} = \Phi\left(-U\left(x_{ig}\right)\right)$. Therefore, with a confidence level α ,
- the upper and lower bounds of \hat{S}_s and \hat{S}_f can be found as:

$$\hat{S}_{s} \in \left(\boldsymbol{\theta}_{\hat{S}_{s}}^{-1}\left(\frac{\alpha}{2}\right), \boldsymbol{\theta}_{\hat{S}_{s}}^{-1}\left(1 - \frac{\alpha}{2}\right)\right) \tag{36}$$

$$\hat{S}_f \in \left(\boldsymbol{\theta}_{\hat{S}_f}^{-1}\left(\frac{\alpha}{2}\right), \boldsymbol{\theta}_{\hat{S}_f}^{-1}\left(1 - \frac{\alpha}{2}\right)\right) \tag{37}$$

where $\boldsymbol{\theta}_{\hat{S}_s}^{-1}$ and $\boldsymbol{\theta}_{\hat{S}_f}^{-1}$ are the inverse CDF of the Poisson binomial distribution. According to Eq. (33), the upper and lower bounds of the total number of failure points can be derived as:

$$N_f \in \left[\widehat{N}_f - \widehat{S}_f^u, \ \widehat{N}_f + \widehat{S}_S^u \right] \tag{38}$$

where \hat{S}_f^u and \hat{S}_s^u are the upper bounds of \hat{S}_f and \hat{S}_s , respectively, thus, the maximum error can be estimated

$$\epsilon = \left| \frac{\widehat{N}_f}{N_f} - 1 \right| \le \max\left(\left| \frac{\widehat{N}_f}{\widehat{N}_f - \widehat{S}_f^u} - 1 \right|, \left| \frac{\widehat{N}_f}{\widehat{N}_f + \widehat{S}_s^u} - 1 \right| \right) = \hat{\epsilon}_{max}$$
 (39)

where $\hat{S}_f^u = \boldsymbol{\theta}_{\hat{S}_f}^{-1} \left(1 - \frac{\alpha}{2}\right)$ and $\hat{S}_s^u = \boldsymbol{\theta}_{\hat{S}_s}^{-1} \left(1 - \frac{\alpha}{2}\right)$. More details for the computation of $\hat{\epsilon}_{max}$ can be found in [29].

• Step 8: Checking the stopping criterion based on the maximum error. Check the stopping criterion:

$$\hat{\epsilon}_{max} \le \epsilon_{thr} \tag{40}$$

where ϵ_{thr} is the error threshold set by researchers. If the stopping criterion is not satisfied, then the process moves to step 3; otherwise, to step 9. It is expected that the true error (denoted as ϵ), with confidence level α , should be smaller than $\hat{\epsilon}_{max}$. The relationships among ϵ , $\hat{\epsilon}_{max}$, and ϵ_{thr} , is:

$$\epsilon \le \hat{\epsilon}_{max} \le \epsilon_{thr}$$
 (41)

It is shown that this error-based stopping criterion successfully solves the unnecessary training problems associated with surrogate-based reliability analysis methods, as their stopping criteria are not directly linked to the extent of error in the estimated failure probability.

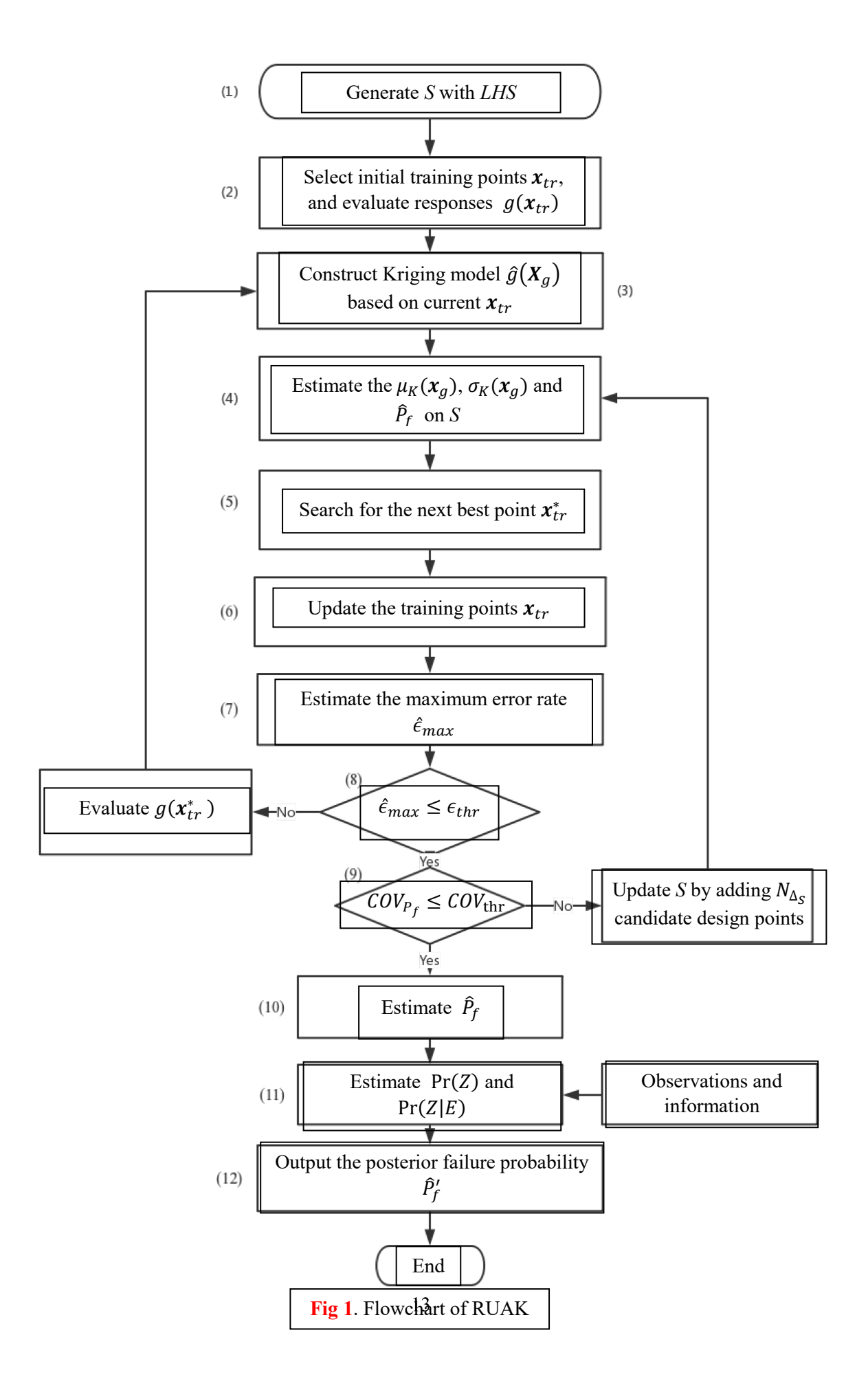
• **Step 9**: *Checking the coefficient of variation of the failure probability*. In this step, the sufficiency of the population of *S* is checked using:

$$COV_{\hat{P}_f} = \sqrt{\frac{1 - \hat{P}_f}{\hat{P}_f N_{MCS}}} \le COV_{thr} \tag{42}$$

where $COV_{\hat{P}_f}$ is the coefficient of variation of \hat{P}_f and COV_{thr} is the corresponding threshold, which is typically adopted as 0.05 [8]. If Eq. (42) is satisfied, then the process moves to step 10. If not, it means that the number of N_{MCS} is insufficient and an additional number $N_{\Delta S}$ of candidate design samples Δ_S should be added to S, and the process should move back to step 4.

- Step 10: Obtain the output of the prior failure probability \hat{P}_f . The estimate of the prior failure probability is final.
- Step 11: Estimate Pr(Z) and Pr(Z|E). In this step, the probability of evidence Pr(Z) and the conditional probability of Pr(Z|E) are computed based on the well-trained surrogate model $\hat{g}(X_g)$ using Eq. (20). Note that the failed samples should be drawn sufficiently based on $\hat{g}(X_g)$ for the purpose of accurate estimate of Pr(Z|E).
- Step 12: Output of the posterior failure probability \widehat{P}'_f . Estimate the posterior failure probability using Eq. (14).

Note that the steps 1-6 in RUAK correspond to similar steps in AK-MCS [8]. In AK-MCS, the inner loop adaptively trains the Kriging model until the stopping criterion ($Max(EFF) \le 0.001$ or $Min(U) \ge 2$) is satisfied based on the current candidate design sample, S. However, the size of S (i.e. N_{MCS}) has influence on the accuracy of the limit state of $\hat{g}(x_g)$, thus, the size of S should be well defined. In the outer loop, a proper number of samples N_{MCS} is selected first. This number may adaptively increase until the stopping criterion in Eq. (42) is satisfied. If the two stopping criteria are satisfied, the Kriging model is regarded as well trained. In RUAK, the stopping criterion for the outer loop is the same as that in AK-MCS. However, the stopping criterion for the inner loop is set based on an upper bound derived in [29] for the error in failure probability estimate given the size of samples in S.



RUAK offers two major advantages compared with conventional reliability updating approaches. First, reliability updating is transformed into three independent regular reliability analysis problems, which can be efficiently analyzed using surrogated-model based reliability analysis methods. Particularly, the numerator in Eq. (13) involves a series system reliability problem and such a problem is typically very rare. In such cases, non-simulation based reliability analysis methods such as FORM and SORM may not offer reliable results. The second important feature of the proposed method is its high efficiency in reliability updating since it does not require investigating the performance function as new information becomes available. It should be noted that two viewpoints can be followed for the estimation of P_f' . The first approach is introduced in this paper, which is the direct application of the Bayes' theorem to reliability updating problem as shown in Eq. (14). Another viewpoint is to first update the distribution of random vector X_g using Bayesian updating procedures based on new information and then estimate P_f' for the system with updated model variables using classical or advanced reliability analysis methods. The latter approach is of course computationally very demanding.

In the Appendix, it is proved that these two general approaches lead to the same estimate of P'_f . In the first approach, which is the basis of the proposed method, the accuracy of the estimated posterior probability of failure mainly relies on the construction of the limit state function. First, it should be noted that there is no error in Pr(Z) since the computations of Pr(Z) in both pure MCS and Kriging-based MCS are the same. Therefore, the error in the estimate of P_f can stem from the computation of P_f and Pr(Z|E). Second, based on Fig.2 (a), it can be inferred that the estimated limit state, $\hat{g}(X_a)$, is very close to the true limit, $g(X_a)$, as the stopping criterion is set appropriately. It can be further inferred that the failure probability estimated by the Kriging-based MCS closely approximates the one estimated through the pure MCS. Thus, the error of P_f can be negligible. Furthermore, as the stopping criterion is set appropriately so that $\hat{g}(X_g) \cong$ $g(X_q)$, the error of Pr(Z|E) becomes negligible. As shown in Fig.2 (a) and (b), let S denote the set of candidate samples. If the responses of these points are examined by the true performance function $g(X_a)$, S can be classified into two groups of points S_s and S_f . Here, S_s means the set of points that are truly safe and S_f denotes the set of points that are truly failure. Then Pr(Z|E) is calculated based on S_f using the approach for computing the probability of equality information. If the aforementioned process is implemented using the Kriging surrogate model, S should be classified into two groups of points $S_s^{'}$ and $S_f^{'}$. Here, $S_s^{'}$ and $S_f^{'}$ denote the set of points that are estimated through the Kriging surrogate model as safe and failure, respectively. Therefore, $S_f^{'}$ can be accurately estimated so that $S_f^{'}\cong S_f$ when the stopping criterion becomes very tight indicating that the limit state is accurately estimated. This process can also ensure the accuracy of Pr(Z|E) as its estimation relies on S_f (Fig.2 (b)).

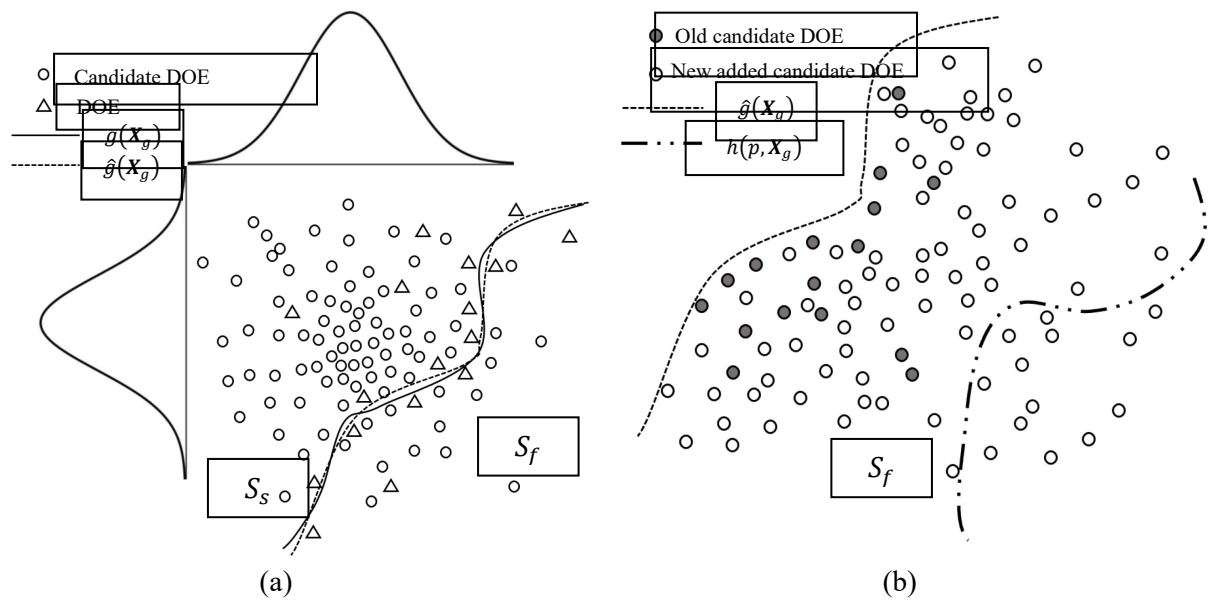


Fig. 2 Illustration of the proposed method: (a) candidate design samples and the true and estimated limit state functions for the estimation of P_f and (b) candidate design samples and the limit state functions for the estimation of Pr(Z|E)

5. Numerical examples

 In this section, four numerical examples representing different levels of complexities, various probabilistic distributions, and different number of dimensions are implemented to explore the efficiency and accuracy of RUAK.

5.1. Low-dimensional example

The first example is two-dimensional and is designed to graphically illustrate the process of the proposed RUAK algorithm. This problem describes the relation between load and load-bearing capacity in the following form [50]:

$$g(R) = R - S \tag{43}$$

where the load S=2.0 is a constant and the capacity R follows the Weibull distribution with the shape parameter k=3.0 and scale parameter v=10. The event E is defined as the set of outcomes in the failure domain $\Omega_f(r)=\{g(r)\leq 0\}$. A measurement of the capacity r_m is available as $r_m=6.0$ with the associated measurement error ε_m , which follows standard normal distribution. Thus, the likelihood function can be represented as:

$$L(r, r_m) = \varphi(r_m - r) \tag{44}$$

where r are the samples from R. In the computation of \hat{P}_f , the threshold of the stopping criterion is set to $\epsilon_{thr} = 0.05$, the coefficient of variation of \hat{P}_f is also set to $COV_{\hat{P}_f} = 0.05$, the number of training samples is initially set as 12, and the initial number of candidate design points for RUAK is $N_S = 10^5$ with $N_{\Delta_S} = 10^5$. The results for prior failure probability with MCS and RUAK are presented in Table 1. Moreover, the limit state function for Pr(Z) can be formulated as:

$$h^{+}(p,r) = p - c_1 L(r, r_m) \tag{45}$$

- where $L(r, r_m)$ is the likelihood of the error with $L(r, r_m) = \varphi(\varepsilon_m)$, $\varphi(\cdot)$ is the PDF of the standard normal distribution and $c_1 = \frac{1}{\max(L(r_i, r_m))}$, $r_i \in S$. Fig.3 (a) illustrates the limit state in $h^+(p, r)$. Note that $\Pr(Z) = \frac{1}{\max(L(r_i, r_m))}$
- $\frac{1}{c_1} \cdot \frac{\sum_{i=1}^{N_{mcs}} I_{Z^+}(p_i, r_i)}{N_{mcs}}, r_i \in S \text{ with:}$

$$I_{Z^{+}}(p_{i}, r_{i}) = \begin{cases} 1, & \text{when } h^{+}(p_{i}, r_{i}) \leq 0 \\ 0, & \text{when } h^{+}(p_{i}, r_{i}) > 0 \end{cases}, r_{i} \in S$$

$$(46)$$

The limit state function for the conditional probability of the evidence Pr(Z|E) can be presented as:

$$h^{++}(p,r') = p - c_2 L(r',r_m) \tag{47}$$

- where r' are the samples with posterior distribution of R in Ω_f and $c_2 = \frac{1}{\max(L(r'_i, r_m))}$, $r'_j \in \hat{S}_f$. Moreover,
- $\Pr(Z|E) = \frac{1}{c_2} \cdot \frac{\sum_{j=1}^{N_f} I_{Z^{++}}(p_i, r'_j)}{\hat{N}_f}, r'_j \in \hat{S}_f \text{ with:}$

$$I_{Z^{++}}(p_i, r_j') = \begin{cases} 1, & \text{when } h^{++}(p_i, r_j') \le 0\\ 0, & \text{when } h^{++}(p_i, r_j') > 0 \end{cases}, r_j' \in \hat{S}_f$$

$$(48)$$

The limit state function $h^{++}(p, r')$ is illustrated in Fig. 3 (b). It is shown that only the points estimated as failure in g(r) remain in estimating the conditional probability Pr(Z|E). Because of the difference between constants c_1 and c_2 , the limit states in $h^+(p,r)$ and $h^{++}(p,r')$ are different.

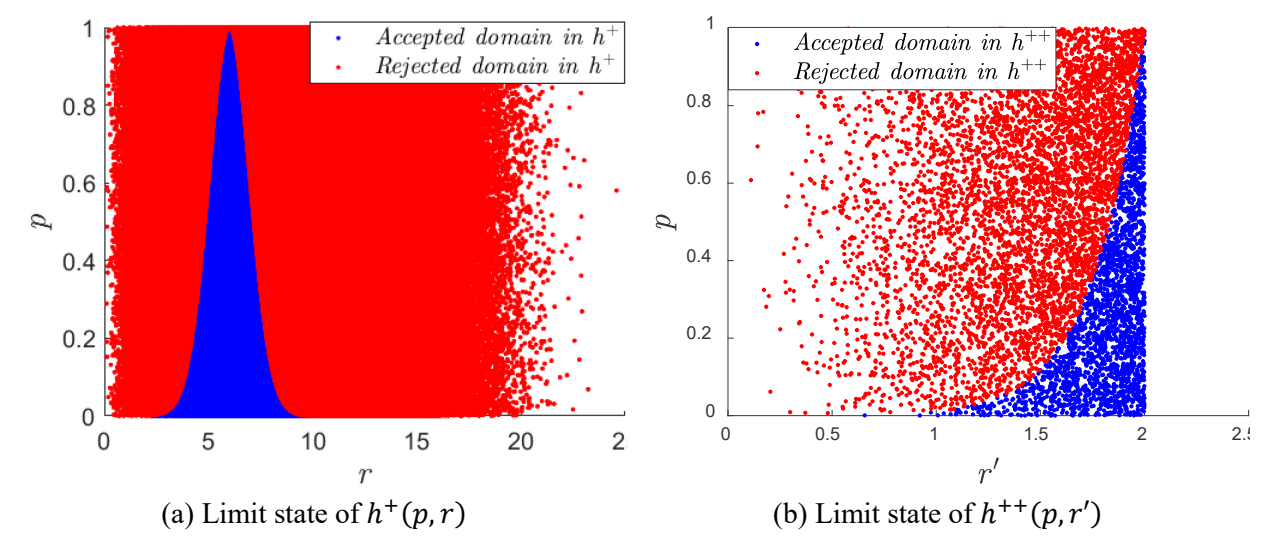


Fig. 3 Illustration of $h^+(p,r)$ and $h^{++}(p,r')$

Table 1. Reliability updating results for Example 1 based on 10 simulations. For the purpose of comparison, results from [50] including the Axis-Parallel Importance Sampling (APIS), FORM/SORM are also summarized here. Note that N_{call} denotes the number of calls to the performance function and N_{ls} ($N_{ls} \ge 1$) is the number of calls for one line search in APIS.

Methodology	$\widehat{P_f^{'}}$	\widehat{P}_f	Computational demand
MCS	$[3.49, 3.70] \times 10^{-6}$	$[7.86, 8.10] \times 10^{-3}$	$N_{call} = 1 \times 10^6$
RUAK (DACE & $\epsilon_{thr} = 0.05$)	$[3.36, 3.87] \times 10^{-6}$	$[7.75, 8.21] \times 10^{-3}$	$N_{call} = 12$
RUAK (DACE & $\epsilon_{thr} = 0.01$)	$[3.42, 3.81] \times 10^{-6}$	$[7.79, 8.20] \times 10^{-3}$	$N_{call} = 12$
RUAK (UQLab & $\epsilon_{thr}=0.05$)	$[3.21, 3.96] \times 10^{-6}$	$[7.62, 8.42] \times 10^{-3}$	$N_{call} = 12$
RUAK (UQLab & $\epsilon_{thr} = 0.01$)	$[3.45, 3.76] \times 10^{-6}$	$[7.79, 8.17] \times 10^{-3}$	$N_{call} = 12{\sim}14$
APIS [50]	$[2.95, 3.91] \times 10^{-6}$	-	$N_{call} = 500 \times N_{ls}$
FORM [50]	1.37×10^{-6}	-	-
SORM [50]	2.11×10^{-6}	-	<u>-</u>

Two toolboxes for Kriging including DACE [69], [73] and UQLab [68] are investigated to explore the performance of RUAK. When implementing these two toolboxes, the Gaussian kernel function and ordinary Kriging are chosen. Moreover, the gradient algorithm is implemented for the global optimization in UQLab toolbox. To satisfy $COV_{\tilde{P}_f} \leq COV_{thr} = 0.05$ as mentioned in step 9 of RUAK, the final number of candidate design samples is determined as 1×10^5 (i.e. $N_{mcs} = 1 \times 10^5$). The results in Table 1 showcase that the proposed algorithm RUAK outperforms other methods in terms of accuracy and efficiency. As the stopping criterion for training the Kriging surrogate model becomes tight (i.e. ϵ_{thr} changes from 0.05 to 0.01), the estimated prior and posterior failure probability become closer to the results obtained by the MCS. When $\epsilon_{thr} = 0.01$, the results estimated using UQlab toolbox is more accurate than DACE even though implementation using UQLab requires fewer number of evaluations of the performance function. The performance of FORM/SORM based on Eq. (13) is not satisfactory because $Pr(E \cap Z)$ is a very rare joint event for which it is very difficult to find the MPP. Moreover, even though the sample-based approach APIS can reach acceptable results, it requires a relatively large number of evaluations of g(R). Compared with the approaches above, the proposed RUAK algorithm needs only 6 evaluations of g(R) and also achieves very high accuracy in both prior and posterior failure probabilities.

5.2. Linear and normal case

The second example is selected to investigate the performance of reliability updating methods for a problem involving multiple random variables [50]. The performance function is defined as:

$$g(X_g) = 2X_1 + 3X_2 + 6X_3 + 4X_4 - X_5 - 2X_6 - 4X_7 - 4X_8$$
(49)

where $X_g = [X_1, ..., X_8]$ are identically distributed independent normal random variables with mean $\mu_X = 10$ and standard deviation $\sigma_X = 2$. Three observations are made in this example with three measurement errors ε_{m1} , ε_{m2} , and ε_{m3} . All of those are identical independent standard normal random variables.

$$L(\mathbf{x}) = \prod_{i=1}^{3} L_i(x_i, x_{i+1}) = \prod_{i=1}^{3} \varphi(20 - x_i - x_{i+1})$$
 (50)

where x_1, x_2, x_3 , and x_4 are samples from X_1, X_2, X_3 , and X_4 . In the implementation of RUAK for computing \hat{P}_f , the threshold of the stopping criterion is set to $\epsilon_{thr} = 0.05$, the coefficient of variation of \hat{P}_f is also set to $COV_{\hat{P}_f} = 0.05$, the number of initial training samples is set to 12, and the initial number of candidate design points for RUAK is $N_S = 10^4$ with $N_{\Delta_S} = 10^4$. The results obtained using RUAK are presented in Table 2. Note that the limit state function $h^+(p, x_q)$ for the probability of evidence Pr(Z) is:

$$h^+(p, \mathbf{x}_g) = p - c_1 L(\mathbf{x}_g) \tag{51}$$

where the likelihood function $L(x_g) = \varphi(\varepsilon_{m1}) \cdot \varphi(\varepsilon_{m2}) \cdot \varphi(\varepsilon_{m3})$ and $c_1 = \frac{1}{\max(L(x_i))}$, $x_i \in S$. Similarly, the limit state function for the conditional probability of the evidence $\Pr(Z|E)$ can be represented as:

$$h^{++}(p, x') = p - c_2 L(x')$$
(52)

where \mathbf{x}' s are the samples from the posterior distribution of \mathbf{X}_g in Ω_f and $c_2 = \frac{1}{\max(L(\mathbf{x}'_i))}$, $\mathbf{x}'_j \in \hat{S}_f$.

Table 2. Reliability updating results for Example 2 based on 10 simulations. For the purpose of comparison, results from [50] including APIS and FORM/SORM are also summarized here.

Methodology	$\widehat{P_f^{'}}$	\widehat{P}_f	Computational demand
MCS	$[0.82, 1.08] \times 10^{-3}$	$[2.36, 2.40] \times 10^{-2}$	$N_{call} = 1 \times 10^6$
RUAK (DACE & $\epsilon_{thr} = 0.05$)	$[0.79, 1.21] \times 10^{-3}$	$[2.21, 2.52] \times 10^{-2}$	$N_{call} = 69{\sim}88$
RUAK (DACE & $\epsilon_{thr} = 0.01$)	$[0.81, 1.14] \times 10^{-3}$	$[2.32, 2.44] \times 10^{-2}$	$N_{call}=115{\sim}158$
RUAK (UQLab & $\epsilon_{thr}=0.05$)	$[0.81, 1.17] \times 10^{-3}$	$[2.26, 2.48] \times 10^{-2}$	$N_{call} = 39{\sim}54$
RUAK (UQLab & $\epsilon_{thr}=0.01$)	$[0.83, 1.12] \times 10^{-3}$	$[2.35, 2.43] \times 10^{-2}$	$N_{call} = 75{\sim}93$
APIS [50]	$[1.00, 1.30] \times 10^{-3}$	-	$N_{call} \cong 1 \times 10^4$
FORM [50]	0.22×10^{-3}	-	-
SORM [50]	1.60×10^{-3}	-	

The performance of RUAK is summarized in Table 2, which examines its implementation with two Kriging toolboxes including DACE [69], [73] and UQLab [68]. In this case, the final number of candidate design samples is determined as 2×10^4 (i.e., $N_{mcs} = 2 \times 10^4$). It is shown that N_{call} when using DACE is significantly larger than that for UQLab. Specifically, N_{call} ranges from 69 to 88 for DACE, while it ranges from 39 to 54 for UQLab for ϵ_{thr} of 0.05. Moreover, N_{call} is in the range of 115-158 for DACE with 10 simulations, while it ranges from 75 to 93 using UQLab for ϵ_{thr} of 0.01. Generally, the estimated posterior probability of failure, \hat{P}_f' , appears to be close to the results obtained using MCS as ϵ_{thr} becomes tighter. When ϵ_{thr} is equal to 0.05 and 0.01, the estimates of \hat{P}_f' are in the range [0.81,1.14] \times 10⁻³ and [0.83,1.10] \times 10⁻³, respectively using UQLab. For DACE, these estimates are in the range [0.79,1.21] \times 10⁻³ and [0.81,1.14] \times 10⁻³, respectively for ϵ_{thr} of 0.05 and 0.01. The estimates \hat{P}_f' using MCS are in the range [0.82,1.08] \times 10⁻³. These results indicate that UQLab toolbox is more accurate, robust and efficient than DACE. This is due to the fact that UQLab uses global optimization to determine the hyper-parameters, while the DACE toolbox uses a local optimization method. The estimated posterior failure probability using FORM and SORM generates an error of nearly 50% compared with MCS. This

demonstrates that FORM and SORM are not appropriate for this problem. Additionally, APIS requires approximately 10^4 evaluations of the performance function $g(X_g)$. However, the proposed RUAK method can achieve both high accuracy and efficiency compared with those approaches with maximum of 88 evaluations of the performance function.

5.3. Structural system case

The third example is a classical structural system studied by many researchers [58], [74]. As shown in Fig. 4, this elastoplastic frame is subjected to both horizontal load H and vertical load V. The plastic-moment capacities of this structure are denoted by $R_1, R_2, ..., R_5$. This example investigates a series system reliability problem because of three failure mechanisms including sway, beam, and combined mechanisms. Thus, the response of the performance function can be defined as the minimum of three corresponding responses as follows:

 $g(v, h, \mathbf{r}) = min \begin{cases} r_1 + r_2 + r_4 + r_5 - 5h \\ r_2 + 2r_3 + r_4 - 5v \\ r_1 + 2r_3 + 2r_4 + r_5 - 5h - 5v \end{cases}$ (53)

where H follows the Gumbel distribution, V follows the Gamma distribution and $R_1, R_2, ..., R_5$ are correlated and lognormally distributed. The probabilistic information of random variables is summarized in Table 3.

Table 3. Random variables in Example 3.

Random variable	Distribution type	Mean	C.O.V	Correlation
$R_i, i = 1, \dots, 5(kN.m)$	Joint lognormal	150	0.2	$\rho_{\ln R} = 0.3$
H(kN)	Gumbel	50	0.4	Independent
V (kN)	Gamma	60	0.2	Independent

Two measurements for R_4 and R_5 , denoted as M_4 and M_5 , are available with measuring errors ε_{m1} and ε_{m2} following independent normal distributions with mean 0 and standard deviation of 15 kN. m. Thus, the likelihood function can be represented as:

$$L(\mathbf{r}) = \varphi^*(M_4 - r_4) \cdot \varphi^*(M_5 - r_5) \tag{54}$$

where r_4 and r_5 are samples from R_4 and R_5 , and φ^* is the PDF of normal distribution with mean 0 and standard deviation of 15 kN. m. In the implementation of RUAK, the number of initial training samples is set to 12 and the initial number of candidate design points is $N_S = 10^4$ with $N_{\Delta_S} = 10^4$. The results of this case are presented in Table 4.

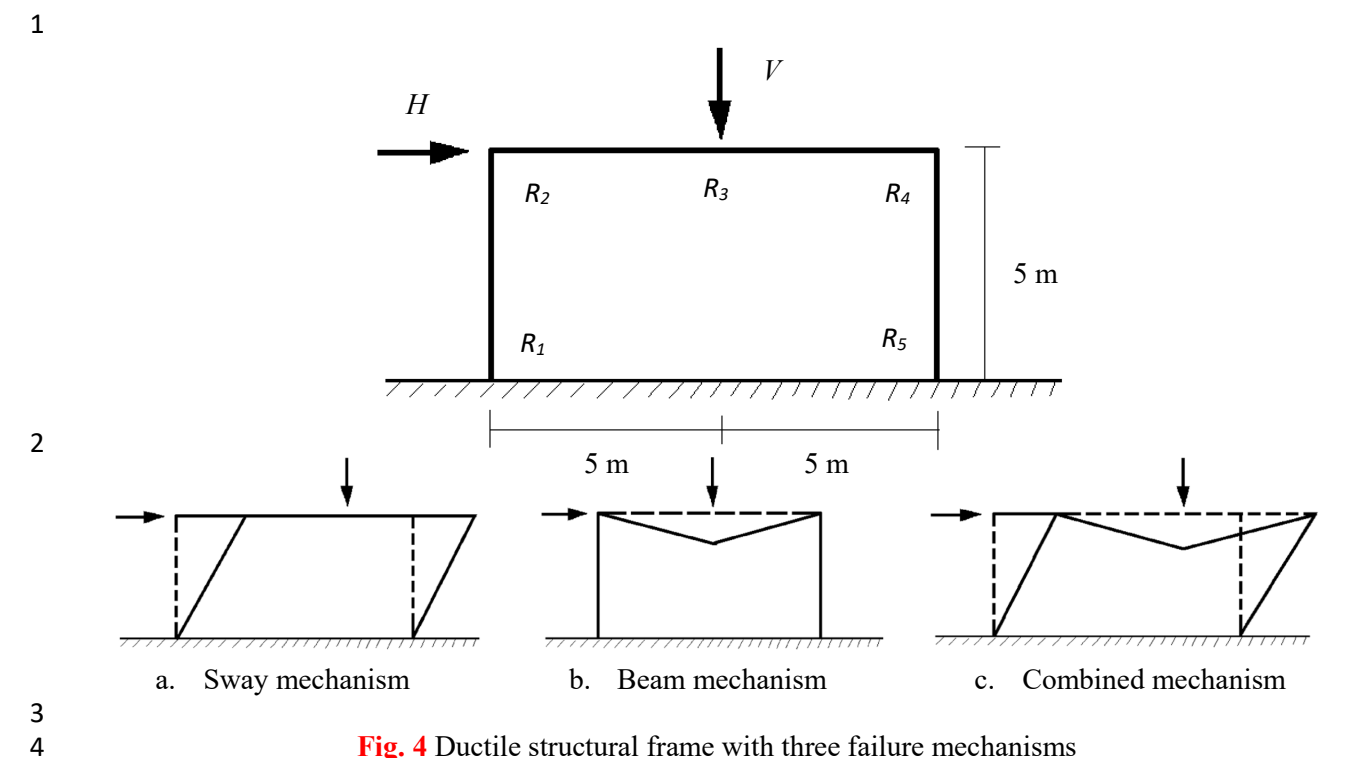


Fig. 4 Ductile structural frame with three failure mechanisms

The limit state function $h^+(p, \mathbf{r})$ for the probability of evidence Pr(Z) is:

5 6

7

8 9

10

11

12

13 14

15

16

17

18

19

20

21

22 23

24

25

26

$$h^+(p, \mathbf{r}) = p - c_1 L(\mathbf{r}) \tag{55}$$

where the likelihood function $L(\mathbf{r}) = \varphi(\varepsilon_{m1}) \cdot \varphi(\varepsilon_{m2})$ and $c_1 = \frac{1}{\max(L(\mathbf{r}_i))}, \mathbf{r}_i \in S$. Similarly, the limit state function for the conditional probability of evidence Pr(Z|E) can be presented as:

$$h^{++}(p, \mathbf{r}') = p - c_2 L(\mathbf{r}') \tag{56}$$

where r's are the samples with a posterior distribution of R in Ω_f and $c_2 = \frac{1}{\max(L(r'_i))}, r'_j \in \hat{S}_f$.

As shown in Table 4, the proposed RUAK algorithm is very efficient in reducing the computational demand compared with the eBN/rBN approach. For computing the potential tables in the reduced BNs, 441 times of structural reliability analyses are needed, each requiring often more than tens of calls to the performance function. In terms of accuracy of \hat{P}_f , both eBN/rBN and RUAK have good performance. The discretization of continuous points in reduced BNs and construction of the potential table are among reasons for the large number of N_{call} . Moreover, the eBN/rBN approach requires expert knowledge to construct an efficient BN. However, this process is completely avoided in the proposed RUAK algorithm. In this example, two Kriging toolboxes including DACE [69], [73] and UQLab [68] are implemented. The final number of candidate design samples is determined as 2×10^4 (i.e., $N_{mcs} = 2 \times 10^4$). As shown in Table 4, DACE toolbox requires a larger number of calls to the performance function compared to UQLab. For this example, one should note that three groups of information (i.e., $M_4 = 50$ and $M_5 = 100$, $M_4 = 150$ and $M_5 = 100$, and $M_4 = 150$ and $M_5 = 200$) are used to update the reliability. For conventional reliability updating methods such as the eBN/rBN method in [50], the total number of calls to the performance function increases corresponding to the number of different groups of information. However, this is not the case in RUAK because of the well-trained surrogate model and the independent estimation

of the prior probability of failure. These features can greatly benefit real-time health monitoring and warning systems that need to investigate sophisticated models rapidly.

Table 4. Reliability updating results for Example 3 based on 10 simulations. For the purpose of comparison, results from eBN/rBN in [58] are also summarized here. Note that $N_{SRA}(N_{SRA} \ge 1)$ is the number of evaluations of the performance function for one structural reliability analysis in eBN/rBN.

	$\widehat{P_f}^{'}$	$\widehat{P_f}^{'}$	$\widehat{P_f}^{'}$		
Methodology	$(M_4 = 50)$ $M_5 = 100)$	$(M_4 = 150)$ $M_5 = 100)$	$M_4 = 150$ $M_5 = 200$	\widehat{P}_f	Computational demand
MCS	[2.35, 2.72] $\times 10^{-1}$	[3.51, 3.68] × 10^{-2}	$ \begin{array}{c} [6.51, 7.75] \\ \times 10^{-3} \end{array} $	[2.53, 2.75] × 10^{-2}	$N_{call} = 1 \times 10^6$
RUAK	[2.19, 2.98]	[3.28, 3.82]	[6.28, 7.96]	[2.39, 2.91]	$N_{call} = 94 \sim 144$
(DACE & $\epsilon_{thr} = 0.05$) RUAK	$\times 10^{-1}$ [2.23, 2.84]	$\times 10^{-2}$ [3.33, 3.78]	$\times 10^{-3}$ [6.33, 7.81]	$\times 10^{-2}$ [2.57, 2.85]	
(DACE & $\epsilon_{thr} = 0.01$)	$\times 10^{-1}$	$\times 10^{-2}$	$\times 10^{-3}$	$\times 10^{-2}$	$N_{call} = 225 \sim 275$
RUAK (UQLab & $\epsilon_{thr} = 0.05$)	$[2.19, 2.94]$ $\times 10^{-1}$	[3.31, 3.79] $\times 10^{-2}$	$[6.29, 7.95] \times 10^{-3}$	[2.38, 2.87] × 10^{-2}	$N_{call} = 64 \sim 93$
RUAK	[2.27, 2.82] × 10^{-1}	[3.38, 3.75] $\times 10^{-2}$	[6.38, 7.78] × 10^{-3}	[2.55, 2.81] × 10^{-2}	$N_{call} = 187 \sim 214$
(UQLab & $\epsilon_{thr} = 0.01$) eBN/rBN [58]	2.4×10^{-1}	3.6×10^{-2}	7.1×10^{-3}	$\times 10^{-2}$ 2.6×10^{-2}	$N_{call} = 441 \times N_{SRA}$

5.4. Example with 10 dimensions

The fourth example investigates a 23-bar truss with 10 input random variables [9], [72]. This example is designed here to investigate the capability of the proposed RUAK algorithm in working on multiple measurements. As shown in Fig. 5, the structure includes 11 horizontal bars and 12 diagonal bars and is subjected to 6 vertical forces $P = [P_1, ..., P_6]$. The performance function of this problem is defined as:

$$g(\mathbf{P}, A_1, A_2, E_1, E_2) = 0.14 - |dis(\mathbf{P}, A_1, A_2, E_1, E_2)|$$
(57)

where $dis(P, A_1, A_2, E_1, E_2)$ is the displacement at the midpoint m and can be calculated using structural analysis methods. The vertical forces P_1 to P_6 all follow Gumbel distributions. A_1 and A_2 are the cross section of horizontal and diagonal bars, respectively, and E_1 and E_2 are their Young's moduli. The probabilistic information of the 10 independent random variables is presented in Table 5. In the implementation of RUAK, the number of initial training samples is set to 12 and the initial number of candidate design points for RUAK is $N_S = 10^4$ with $N_{\Delta S} = 10^4$. Four measurements of P_1, P_2, A_1 and A_2 are made with errors ε_{m1} and ε_{m2} , which follow a normal distribution with mean 0 and standard deviation 0.5×10^4 and ε_{m3} and ε_{m4} , which follow a normal distribution with mean 0 and standard deviation 1×10^{-4} . Thus, the likelihood function can be represented as:

$$L(\mathbf{x}) = \varphi^{1,2}(\varepsilon_{m1}) \cdot \varphi^{1,2}(\varepsilon_{m2}) \cdot \varphi^{3,4}(\varepsilon_{m3}) \cdot \varphi^{3,4}(\varepsilon_{m4})$$

$$= \varphi^{1,2}(8.5 \times 10^4 - P_1) \cdot \varphi^{1,2}(7.5 \times 10^4 - P_6) \cdot \varphi^{3,4}(1.85 \times 10^{-3} - A_1)$$

$$\cdot \varphi^{3,4}(0.9 \times 10^{-3} - A_2)$$
(58)

where $\varphi^{1,2}$ is the PDF of normal distribution with mean 0 and standard deviation 0.5×10^4 and $\varphi^{3,4}$ is the PDF of normal distribution with mean 0 and standard deviation 1×10^{-4} . The limit state function $h^+(p, x_g)$ for the probability of evidence Pr(Z) is:

$$h^{+}(p, \mathbf{x}_{q}) = p - c_{1}L(\mathbf{x}_{q}) \tag{59}$$

where p are the samples from the standard uniform distribution, $x_g = [p_1, p_6, a_1, a_2]$ and $c_1 = \frac{1}{\max(L(x_i))}$, $x_i \in S$.

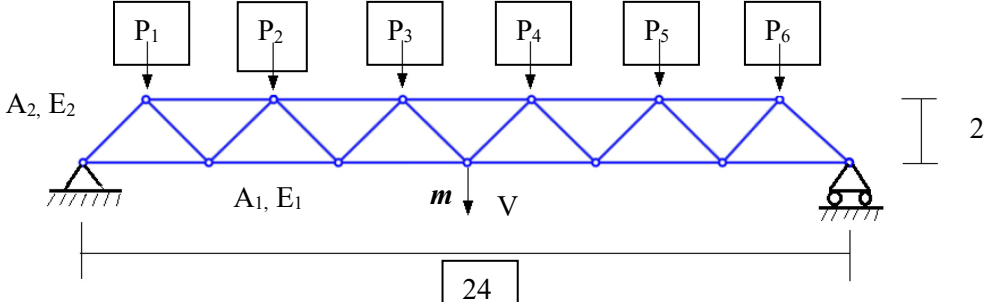


Fig. 5 Example 4, truss with 10 random variables

Table 5. Random variables in Example 4.

	Random variable	Distribution	Mean	Standard deviation
	$P_1 - P_6$	Gumbel	6.5×10^{4}	6.5×10^{3}
	A_1	Lognormal	2×10^{-3}	2×10^{-4}
	A_2	Lognormal	1×10^{-3}	1×10^{-4}
	$\overline{E_1}$	Lognormal	2.1×10^{11}	2.1×10^{11}
_	$\overline{E_2}$	Lognormal	2.1×10^{11}	2.1×10^{11}

Similarly, the limit state function for the conditional probability of evidence Pr(Z|E) can be presented as:

$$h^{++}(p, \mathbf{x}') = p - c_2 L(\mathbf{x}') \tag{60}$$

where \mathbf{x}' are the samples from the posterior distribution of \mathbf{X}_g in Ω_f and $c_2 = \frac{1}{\max(L(\mathbf{x}_j))}, \mathbf{x}_j' \in \hat{S}_f$. The

simulation results are summarized in Table 6.

 In this example, it is shown that the number of evaluations of the Finite Element model using MCS is quite large. Moreover, the estimates of the prior and posterior failure probabilities using the proposed method are accurate. The final number of candidate design samples for this example is determined as 5×10^4 (i.e. $N_{mcs} = 5 \times 10^4$). As shown in Table 6, the UQLab toolbox is more efficient than DACE in terms of the number of calls to the performance function. In order to achieve even a higher accuracy in failure probability estimates, the proposed RUAK algorithm offers two options: setting a tighter threshold for error ϵ_{thr} in Eq. (40) and a tighter threshold for the coefficient of variation COV_{thr} in Eq. (42).

Table 6. Reliability updating results Example 4 using RUAK based on 10 simulations.

Methodology $\hat{p}_{f}^{'}$		\widehat{P}_f	Computational demand
MCS	$[0.99, 1.39] \times 10^{-2}$	$[8.38, 8.69] \times 10^{-3}$	$N_{call} = 1 \times 10^6$
RUAK (DACE & $\epsilon_{thr} = 0.05$)	$[0.87, 1.65] \times 10^{-2}$	$[8.16, 8.92] \times 10^{-3}$	$N_{call}=152{\sim}188$
RUAK (DACE & $\epsilon_{thr} = 0.01$)	$[0.93, 1.57] \times 10^{-2}$	$[8.22, 8.84] \times 10^{-3}$	$N_{call} = 235 \sim 275$
RUAK (UQLab & $\epsilon_{thr} = 0.05$)	$[0.86, 1.63] \times 10^{-2}$	$[8.16, 8.89] \times 10^{-3}$	$N_{call}=125{\sim}141$
RUAK (UQLab & $\epsilon_{thr} = 0.01$)	$[0.92, 1.52] \times 10^{-2}$	$[8.25, 8.82] \times 10^{-3}$	$N_{call} = 194{\sim}223$

6. Conclusions

This paper proposes a reliability-updating algorithm named RUAK to estimate the posterior failure probability with equality information using a surrogate model. Different from the approaches in [50] that requires estimation of the probability of an often very rare joint event, the proposed algorithm applies the Bayes' theorem to decompose the posterior failure probability into three parts: prior failure probability, probability of information, and conditional probability of information. This decomposition leads to events with higher probability of occurrence than the joint event in [50]; therefore, decreasing the computational demand of reliability updating. Another important feature is that RUAK leverages surrogate models in general and adaptive Kriging algorithms in particular to estimate the prior failure probability. This well-trained surrogate model in the developed formulation of reliability updating also facilitates estimation of the conditional probability of equality information. This subsequently results in a highly efficient reliability updating algorithm that does not require analyzing originally time-demanding performance functions when new information becomes available. Last but not least, the implementation of RUAK is relatively easy without any empirical knowledge or expertise. Though the adaptive Kriging approach is implemented in the proposed RUAK algorithm, other surrogate models such as the Polynomial Chaos Expansion, Response Surface, and Support Vector Regression are also applicable.

Four numerical examples are investigated to show the advantages of the proposed RUAK algorithm. It is shown that the number of evaluations of those computational examples is significantly reduced through the use of RUAK. However, the application of RUAK is currently appropriate for time-independent cases. Extension of this method for time-dependent reliability updating problems is a future research direction.

Appendix

Two viewpoints toward estimating the posterior probability of failure, P'_f , are illustrated in Fig. 6 and investigated in this section. It is proved that both methods lead to the same posterior probability of failure.

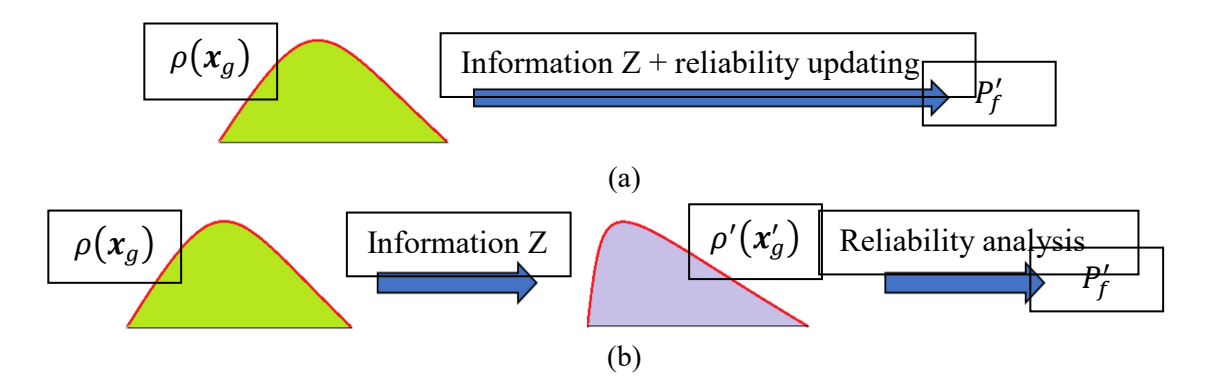


Fig. 6 Two viewpoints toward estimating the posterior probability of failure with (a) estimating P'_f directly using reliability updating algorithm and (b) updating the probability distribution of random variables then implementing a reliability analysis method to estimate P'_f

As introduced in this paper, the first approach estimates the probability of information as shown in Eq. (14). Following the estimation of Pr(Z), Pr(E) and Pr(Z|E) as shown in this paper, the posterior probability can be found as,

$$P_f' = \frac{\int_{x_g \in \Omega_Z} \rho(x_g) dx_g \cdot \int_{x \in \Omega_E} \rho(x_g) dx_g}{\int_{x_g \in \Omega_Z} \rho(x_g) dx_g}$$
(61)

- 1 The second approach is to update the posterior distribution of x first, then reevaluate the probability of
- 2 failure P'_f .

8

12

14

$$\Pr(E|\mathbf{X}'_g) = P'_f = P(g(\mathbf{X}'_g) \le 0) = \int_{\mathbf{X}'_g \in \Omega_E} \rho'(\mathbf{X}'_g) d\mathbf{X}'_g$$
 (62)

- where X'_g denotes the posterior distribution of x_g based on new information. First, the probability density function of X'_g can be represented as,
 - $\rho'(x'_g) = \frac{L(x'_g)\rho(x'_g)}{\int_{X'_g} L(x'_g)\rho(x'_g) dx'_g}$ (63)
- The Bayesian Updating with Structural reliability method (BUS) can be applied here to estimate $\rho'(x'_g)$ [67]:
 - $\rho'(x'_g) = \frac{\rho(x_g | x_g \in \Omega_Z)}{\int_{x_g \in \Omega_Z} \rho(x_g) dx_g}$ (64)
- 9 where $\Omega_{Z} = [p \le cL(\mathbf{x}_{a})] \tag{65}$
- Let C_d denote the constant outcome of the denominator, $\int_{x \in \Omega_Z} \rho(x) dx$. Then Eq. (62) can be further expanded to:
 - $P_f' = \int_{\mathbf{x}_g \in \Omega_E} \rho'(\mathbf{x}'_g) \, d\mathbf{x}'_g = \int_{\mathbf{x}_g \in [\Omega_E \cap \Omega_Z]} \frac{\rho(\mathbf{x}_g)}{C_d} d\mathbf{x}_g$ $= \frac{\int_{\mathbf{x}_g \in [\Omega_E \cap \Omega_Z]} \rho(\mathbf{x}_g) \, d\mathbf{x}_g}{C_d} = \frac{\int_{\mathbf{x} \in [\Omega_E \cap \Omega_Z]} \rho(\mathbf{x}_g) \, d\mathbf{x}_g}{\int_{\mathbf{x}_g \in \Omega_Z} \rho(\mathbf{x}_g) \, d\mathbf{x}_g} = \frac{\int_{\mathbf{x}_g \in \Omega_Z} \rho(\mathbf{x}_g) \, d\mathbf{x}_g \cdot \int_{\mathbf{x}_g \in \Omega_Z} \rho(\mathbf{x}_g) \, d\mathbf{x}_g}{\int_{\mathbf{x}_g \in \Omega_Z} \rho(\mathbf{x}_g) \, d\mathbf{x}_g}$ (66)
- This result is the same as that in Eq. (61).
- 15 Acknowledgements
- This research has been partly funded by the U.S. National Science Foundation (NSF) through awards CMMI-1333943, 1462183, and 1635569. Any opinions, findings, and conclusions or recommendations
- 18 expressed in this paper are those of the authors and do not necessarily reflect the views of the National
- 19 Science Foundation.
 - References
- 22 [1] R. Y. Rubinstein and D. P. Kroese, Simulation and the Monte Carlo method. John Wiley & Sons, 2016.
- 23 [2] G. Fishman, Monte Carlo: concepts, algorithms, and applications. Springer Science & Business Media, 2013.
- R. Rackwitz and B. Flessler, "Structural reliability under combined random load sequences," *Comput. Struct.*, vol. 9, no. 5, pp. 489–494, Nov. 1978.
- [4] Kiureghian Armen Der and Stefano Mario De, "Efficient Algorithm for Second-Order Reliability Analysis," *J. Eng. Mech.*, vol. 117, no. 12, pp. 2904–2923, Dec. 1991.

1 [5] B. Echard, N. Gayton, M. Lemaire, and N. Relun, "A combined importance sampling and kriging reliability method for small failure probabilities with time-demanding numerical models," *Reliab. Eng. Syst. Saf.*, vol. 111, pp. 232–240, 2013.

- [6] S. K. Au and J. L. Beck, "A new adaptive importance sampling scheme for reliability calculations," *Struct. Saf.*, vol. 21, no. 2, pp. 135–158, 1999.
- [7] S. K. Au and J. L. Beck, "Subset simulation and its application to seismic risk based on dynamic analysis," *J. Eng. Mech.*, vol. 129, no. 8, pp. 901–917, 2003.
- 8 [8] B. Echard, N. Gayton, and M. Lemaire, "AK-MCS: an active learning reliability method combining Kriging and Monte Carlo simulation," *Struct. Saf.*, vol. 33, no. 2, pp. 145–154, 2011.
- [9] N. Roussouly, F. Petitjean, and M. Salaun, "A new adaptive response surface method for reliability analysis,"
 Probabilistic Eng. Mech., vol. 32, pp. 103–115, Apr. 2013.
- 12 [10] Faravelli Lucia, "Response-Surface Approach for Reliability Analysis," *J. Eng. Mech.*, vol. 115, no. 12, pp. 2763–2781, Dec. 1989.
 - [11] J.-M. Bourinet, "Rare-event probability estimation with adaptive support vector regression surrogates," *Reliab. Eng. Syst. Saf.*, vol. 150, pp. 210–221, 2016.
 - [12] Schöbi R., Sudret B., and Marelli S., "Rare Event Estimation Using Polynomial-Chaos Kriging," *ASCE-ASME J. Risk Uncertain. Eng. Syst. Part Civ. Eng.*, vol. 3, no. 2, p. D4016002, Jun. 2017.
 - [13] M. Rahimi, Z. Wang, A. Shafieezadeh, D. Wood, and E. J. Kubatko, "Exploring Passive and Active Metamodeling-based Reliability Analysis Methods for Soil Slopes: A New Approach to Active Training," *Int. J. Geomech.*, 2019.
 - [14] Rahimi Mehrzad, Wang Zeyu, Shafieezadeh Abdollah, Wood Dylan, and Kubatko Ethan J., "An Adaptive Kriging-Based Approach with Weakly Stationary Random Fields for Soil Slope Reliability Analysis," *Geo-Congr.* 2019, pp. 148–157.
 - [15] B. J. Bichon, M. S. Eldred, L. P. Swiler, S. Mahadevan, and J. M. McFarland, "Efficient global reliability analysis for nonlinear implicit performance functions," *AIAA J.*, vol. 46, no. 10, pp. 2459–2468, 2008.
 - [16] X. Huang, J. Chen, and H. Zhu, "Assessing small failure probabilities by AK-SS: an active learning method combining Kriging and subset simulation," *Struct. Saf.*, vol. 59, pp. 86–95, 2016.
 - [17] Z. Hu and X. Du, "Mixed Efficient Global Optimization for Time-Dependent Reliability Analysis," *J. Mech. Des.*, vol. 137, no. 5, pp. 051401-051401-9, May 2015.
 - [18] Z. Lv, Z. Lu, and P. Wang, "A new learning function for Kriging and its applications to solve reliability problems in engineering," *Comput. Math. Appl.*, vol. 70, no. 5, pp. 1182–1197, Sep. 2015.
 - [19] Z. Sun, J. Wang, R. Li, and C. Tong, "LIF: A new Kriging based learning function and its application to structural reliability analysis," *Reliab. Eng. Syst. Saf.*, vol. 157, pp. 152–165, 2017.
 - [20] X. Yang, Y. Liu, C. Mi, and C. Tang, "System reliability analysis through active learning Kriging model with truncated candidate region," *Reliab. Eng. Syst. Saf.*, vol. 169, pp. 235–241, 2018.
 - [21] H.-M. Qian, H.-Z. Huang, and Y.-F. Li, "A novel single-loop procedure for time-variant reliability analysis based on Kriging model," *Appl. Math. Model.*, vol. 75, pp. 735–748, Nov. 2019.
 - [22] N. Lelièvre, P. Beaurepaire, C. Mattrand, and N. Gayton, "AK-MCSi: A Kriging-based method to deal with small failure probabilities and time-consuming models," *Struct. Saf.*, vol. 73, pp. 1–11, Jul. 2018.
 - [23] Z. Wen, H. Pei, H. Liu, and Z. Yue, "A Sequential Kriging reliability analysis method with characteristics of adaptive sampling regions and parallelizability," *Reliab. Eng. Syst. Saf.*, vol. 153, pp. 170–179, 2016.
 - [24] Z. Wang and A. Shafieezadeh, "A Parallel Learning Strategy for Adaptive Kriging-based Reliability Analysis Methods," 13th International Conference on Applications of Statistics and Probability in Civil Engineering(ICASP13), Seoul, South Korea, May 26-30, 2019.
 - [25] Z. hu and S. Mahadevan, "A Single-Loop Kriging (SILK) Surrogate Modeling for Time-Dependent Reliability Analysis," *J. Mech. Des.*, vol. 138, Apr. 2016.
 - [26] W. Fauriat and N. Gayton, "AK-SYS: An adaptation of the AK-MCS method for system reliability," *Reliab. Eng. Syst. Saf.*, vol. 123, pp. 137–144, 2014.
 - [27] B. Gaspar, A. P. Teixeira, and C. G. Soares, "Adaptive surrogate model with active refinement combining Kriging and a trust region method," *Reliab. Eng. Syst. Saf.*, 2017.
 - [28] Z. Hu and S. Mahadevan, "Global sensitivity analysis-enhanced surrogate (GSAS) modeling for reliability analysis," *Struct. Multidiscip. Optim.*, vol. 53, no. 3, pp. 501–521, Mar. 2016.
- [29] Z. Wang and A. Shafieezadeh, "ESC: an efficient error-based stopping criterion for kriging-based reliability analysis methods," *Struct. Multidiscip. Optim.*, Nov. 2018.
- [30] C. Jiang, H. Qiu, L. Gao, D. Wang, Z. Yang, and L. Chen, "Real-time estimation error-guided active learning
 Kriging method for time-dependent reliability analysis," *Appl. Math. Model.*, vol. 77, pp. 82–98, 2020.

- 1 [31] M. Balesdent, J. Morio, and J. Marzat, "Kriging-based adaptive Importance Sampling algorithms for rare event 2 estimation," Struct. Saf., vol. 44, pp. 1–10, Sep. 2013.
- 3 [32] V. Dubourg, B. Sudret, and F. Deheeger, "Metamodel-based importance sampling for structural reliability 4 analysis," *Probabilistic Eng. Mech.*, vol. 33, pp. 47–57, Jul. 2013. 5 6

8

9

10

11

12

13

14

15

16

17

18

19

20

21

22

23

24

25

26

27

28

29

30 31

32

33

34

35

36

37

38

39

40

41

42

43

44

45

46

47

50

- [33] X. Zhang, L. Wang, and J. D. Sørensen, "AKOIS: An adaptive Kriging oriented importance sampling method for structural system reliability analysis," Struct. Saf., vol. 82, p. 101876, Jan. 2020.
 - [34] W. Chen, C. Xu, Y. Shi, J. Ma, and S. Lu, "A hybrid Kriging-based reliability method for small failure probabilities," Reliab. Eng. Syst. Saf., vol. 189, pp. 31-41, Sep. 2019.
- [35] V. Dubourg, B. Sudret, and J.-M. Bourinet, "Reliability-based design optimization using kriging surrogates and subset simulation," Struct. Multidiscip. Optim., vol. 44, no. 5, pp. 673–690, Nov. 2011.
- [36] N. Pedroni and E. Zio, "An Adaptive Metamodel-Based Subset Importance Sampling approach for the assessment of the functional failure probability of a thermal-hydraulic passive system," Appl. Math. Model., vol. 48, pp. 269– 288, Aug. 2017.
- [37] J. Zhang, M. Xiao, and L. Gao, "An active learning reliability method combining Kriging constructed with exploration and exploitation of failure region and subset simulation," *Reliab. Eng. Syst. Saf.*, vol. 188, pp. 90– 102, Aug. 2019.
- [38] Z. Wang and A. Shafieezadeh, "REAK: Reliability analysis through Error rate-based Adaptive Kriging," Reliab. Eng. Syst. Saf., vol. 182, pp. 33–45, Feb. 2019.
- [39] "UQLab sensitivity analysis user manual," UQLab, the Framework for Uncertainty Quantification. [Online]. Available: http://www.uqlab.com/userguide-reliability. [Accessed: 13-May-2017].
- [40] B. Sudret, "Global sensitivity analysis using polynomial chaos expansions," Reliab. Eng. Syst. Saf., vol. 93, no. 7, pp. 964–979, Jul. 2008.
- [41] Z. Jiang and J. Li, "High dimensional structural reliability with dimension reduction," *Struct. Saf.*, vol. 69, pp. 35–46, 2017.
- [42] Z. Wang and P. Wang, "A Nested Extreme Response Surface Approach for Time-Dependent Reliability-Based Design Optimization," J. Mech. Des., vol. 134, no. 12, pp. 121007-121007-14, Nov. 2012.
- [43] Z. Wang and P. Wang, "A new approach for reliability analysis with time-variant performance characteristics," Reliab. Eng. Syst. Saf., vol. 115, pp. 70–81, Jul. 2013.
- [44] X. Yang, C. Mi, D. Deng, and Y. Liu, "A system reliability analysis method combining active learning Kriging model with adaptive size of candidate points," Struct. Multidiscip. Optim., vol. 60, no. 1, pp. 137–150, Jul. 2019.
- [45] W. Yun, Z. Lu, P. He, Y. Dai, and X. Jiang, "An efficient method for estimating the parameter global reliability sensitivity analysis by innovative single-loop process and embedded Kriging model," Mech. Syst. Signal Process., vol. 133, p. 106288, Nov. 2019.
- [46] Z. Meng, Z. Zhang, D. Zhang, and D. Yang, "An active learning method combining Kriging and accelerated chaotic single loop approach (AK-ACSLA) for reliability-based design optimization," Comput. Methods Appl. Mech. Eng., vol. 357, p. 112570, Dec. 2019.
- [47] J. Li and J. Chen, "Solving time-variant reliability-based design optimization by PSO-t-IRS: A methodology incorporating a particle swarm optimization algorithm and an enhanced instantaneous response surface," Reliab. Eng. Syst. Saf., vol. 191, p. 106580, Nov. 2019.
- [48] M. Rahimi, A. Shafieezadeh, D. Wood, E. J. Kubatko, and N. C. Dormady, "Bayesian calibration of multiresponse systems via multivariate Kriging: Methodology and geological and geotechnical case studies," Eng. Geol., vol. 260, p. 105248, Oct. 2019.
- [49] Z. Wang and A. Shafieezadeh, "Reliability-based Bayesian Updating using Machine Learning," 13th International Conference on Applications of Statistics and Probability in Civil Engineering(ICASP13), Seoul, South Korea, May 26-30, 2019.
- [50] D. Straub, "Reliability updating with equality information," Probabilistic Eng. Mech., vol. 26, no. 2, pp. 254-258, Apr. 2011.
- 48 [51] S. Gollwitzer, B. Kirchgäßner, R. Fischer, and R. Rackwitz, "PERMAS-RA/STRUREL system of programs for 49 probabilistic reliability analysis," Struct. Saf., vol. 28, no. 1, pp. 108–129, Jan. 2006.
 - [52] Straub Daniel, "Stochastic Modeling of Deterioration Processes through Dynamic Bayesian Networks," J. Eng. Mech., vol. 135, no. 10, pp. 1089–1099, Oct. 2009.
- [53] J. Luque and D. Straub, "Reliability analysis and updating of deteriorating systems with dynamic Bayesian 52 53 networks," Struct. Saf., vol. 62, pp. 34-46, Sep. 2016.
- [54] O. Špačková and D. Straub, "Dynamic Bayesian Network for Probabilistic Modeling of Tunnel Excavation 54 55 Processes," Comput.-Aided Civ. Infrastruct. Eng., vol. 28, no. 1, pp. 1–21, Jan. 2013.

- 1 [55] P. A. P. Ramírez and I. B. Utne, "Use of dynamic Bayesian networks for life extension assessment of ageing 2 systems," *Reliab*, *Eng. Syst. Saf.*, vol. 133, pp. 119–136, Jan. 2015.
- 3 [56] M. I. Rafiq, M. K. Chryssanthopoulos, and S. Sathananthan, "Bridge condition modelling and prediction using 4 dynamic Bayesian belief networks," Struct. Infrastruct. Eng., vol. 11, no. 1, pp. 38-50, Jan. 2015. 5 6

8

9

10

11

12

13

14

15

16

17 18

19

20

21

22

23

24

25

26

27

28

29

30

31

32

33 34

35

36

37

38

39

- [57] Straub Daniel and Der Kiureghian Armen, "Bavesian Network Enhanced with Structural Reliability Methods: Methodology," J. Eng. Mech., vol. 136, no. 10, pp. 1248–1258, Oct. 2010.
- [58] Straub Daniel and Der Kiureghian Armen, "Bayesian Network Enhanced with Structural Reliability Methods: Application," J. Eng. Mech., vol. 136, no. 10, pp. 1259–1270, Oct. 2010.
- [59] Bensi Michelle, Kiureghian Armen Der, and Straub Daniel, "Framework for Post-Earthquake Risk Assessment and Decision Making for Infrastructure Systems," ASCE-ASME J. Risk Uncertain. Eng. Syst. Part Civ. Eng., vol. 1, no. 1, p. 04014003, Mar. 2015.
- [60] D. Y. Yang and D. M. Frangopol, "Probabilistic optimization framework for inspection/repair planning of fatigue-critical details using dynamic Bayesian networks," Comput. Struct., vol. 198, pp. 40–50, Mar. 2018.
- [61] J. Hackl and J. Kohler, "Reliability assessment of deteriorating reinforced concrete structures by representing the coupled effect of corrosion initiation and progression by Bayesian networks," Struct. Saf., vol. 62, pp. 12–23,
- [62] S.-H. Lee and J. Song, "Bayesian-network-based system identification of spatial distribution of structural parameters," Eng. Struct., vol. 127, pp. 260–277, Nov. 2016.
- [63] O. Morales-Nápoles and R. D. J. M. Steenbergen, "Large-Scale Hybrid Bayesian Network for Traffic Load Modeling from Weigh-in-Motion System Data," J. Bridge Eng., vol. 20, no. 1, p. 04014059, Jan. 2015.
- [64] I. Papaioannou and D. Straub, "Reliability updating in geotechnical engineering including spatial variability of soil," Comput. Geotech., vol. 42, pp. 44–51, 2012.
- [65] T. Schweckendiek and A. C. W. M. Vrouwenvelder, "Reliability updating and decision analysis for head monitoring of levees," Georisk, vol. 7, no. 2, pp. 110–121, 2013.
- [66] Lee Young-Joo and Song Junho, "System Reliability Updating of Fatigue-Induced Sequential Failures," J. Struct. Eng., vol. 140, no. 3, p. 04013074, Mar. 2014.
- [67] Straub Daniel and Papaioannou Iason, "Bayesian Updating with Structural Reliability Methods," J. Eng. Mech., vol. 141, no. 3, p. 04014134, Mar. 2015.
- [68] "UQLab Kriging (Gaussian process modelling) manual," UQLab, the Framework for Uncertainty Quantification. [Online]. Available: http://www.uqlab.com/userguidekriging. [Accessed: 13-May-2017].
- [69] S. N. Lophaven, H. B. Nielsen, and J. Søndergaard, "DACE-A Matlab Kriging toolbox, version 2.0," 2002.
- [70] S. Marelli, R. Schöbi, and B. Sudret, "UQLab User Manual Structural Reliability (Rare Events Estimation)," p.
- [71] I. Kaymaz, "Application of kriging method to structural reliability problems," Struct. Saf., vol. 27, no. 2, pp. 133– 151, 2005.
- [72] J. Wang, Z. Sun, Q. Yang, and R. Li, "Two accuracy measures of the Kriging model for structural reliability analysis," Reliab. Eng. Syst. Saf., vol. 167, pp. 494–505, Nov. 2017.
- [73] S. N. Lophaven, H. B. Nielsen, and J. Søndergaard, "Aspects of the matlab toolbox DACE," Informatics and Mathematical Modelling, Technical University of Denmark, DTU, 2002.
- 40 [74] "Engineering Design Reliability Handbook," CRC Press, 22-Dec-2004. [Online]. Available: 41 https://www.crcpress.com/Engineering-Design-Reliability-Handbook/Nikolaidis-Ghiocel-42 Singhal/p/book/9780849311802. [Accessed: 18-May-2018].